Spring 5-2022

Investigating Gluonic Operators in Coordinate Space

Wayne Henry Morris III
Old Dominion University, morris3wh@gmail.com

INVESTIGATING GLUONIC OPERATORS IN COORDINATE SPACE

by

Wayne Henry Morris III
B.S. May 2015, James Madison University
M.S. May 2017, Old Dominion University

A Dissertation Submitted to the Faculty of
Old Dominion University in Partial Fulfillment of the
Requirements for the Degree of

DOCTOR OF PHILOSOPHY

PHYSICS

OLD DOMINION UNIVERSITY
May 2022

Approved by:

Anatoly Radyushkin (Director)

John Adam (Member)

Ian Balitsky (Member)

Alexander Gurevich (Member)

Charles Hyde (Member)

ABSTRACT

INVESTIGATING GLUONIC OPERATORS IN COORDINATE SPACE

Wayne Henry Morris III
Old Dominion University, 2022
Director: Dr. Anatoly Radyushkin

In this dissertation, a method of extracting gluon momentum distributions inside hadrons, and particularly nucleons, is developed. In general, the utility and application of performing calculations in coordinate space at the operator level is discussed, and its application to the method of pseudodistributions in the lattice extraction of parton distributions. An introduction to the background field method and other techniques used in the calculation of corrections to gluon operators are provided. Then, an outline of the calculation of the uncontracted gluon bilocal operator at one-loop is given, and the result thereof. Using the result for the gluon bilocal operator restricted to spacelike separations, $z = (0, 0, 0, z_3)$, various projections and contractions are discussed for the spin averaged case, and for the polarization dependent case in a forward nucleon matrix element. Finally, matching relations between pseudodistributions and lightcone distributions are given for the unpolarized gluon distribution and for the polarized gluon distribution. Application of the results in recent actual lattice extractions of gluon PDFs is discussed, and future applications are outlined.

This dissertation is dedicated to the Great Dismal Swamp.

ACKNOWLEDGEMENTS

I would like to send my gratitude to Anatoly Radyushkin for his mentorship and guidance throughout my doctoral program, and to Ian Balitsky for his collaboration and insight.

I would also like to thank the rest of my dissertation committee: John Adam, Alexander Gurevich, Charles Hyde, and the late Mark Havey, for their time and wisdom in the development of this dissertation.

Additionally, I would like to recognize the members of the HadStruc collaboration, whose efforts gave meaning to my doctoral work.

Finally, I would like to extend my deepest appreciation to the faculty and staff at Old Dominion University, whose dedication and efforts make all of this possible.

TABLE OF CONTENTS

Page

LIST OF FIGURES

Figure Page

CHAPTER 1
INTRODUCTION

Hadron structure and the dynamics of strong interactions are subjects of ongoing investigation in the field of nuclear physics, both experimentally and theoretically. While great strides have been made by the collective efforts of physicists and engineers around the world, there is still much to be understood and discovered. The central theoretical techniques employed in modeling the behavior of hadron constituents, now known to be quarks and gluons, evolved out of the constituent quark picture proposed independently by Gell-Mann and Zweig in 1964 [1, 2], who predicted the existence of the up, down, and strange quarks. The known mesons and baryons at the time could all be constructed from combinations of these three quarks in a way that was consistent with their observed quantum numbers.

The parton model, whose name can be attributed to Feynman [3], was a key development in the understanding of hadron structure, and the formulation of a theory of quarks and gluons. A probabilistic picture, formulated by Bjorken and Paschos in 1969 [4, 5], predicted the existence of point-like partons, composing hadrons, described by the now famous parton distribution functions (PDFs). A PDF, in this framework, describes the probability of finding a parton at some fraction of the longitudinal momentum of its parent hadron. Another approach, developed by Bjorken, led to the prediction of Bjorken scaling. Its essence is that at high energies the nucleon structure functions would be independent of energy for a wide range of energies. The explanation behind this prediction was that the constituent partons could be treated as approximately free at high energies, or correspondingly short distances. Bjorken scaling was confirmed around the same time that it was predicted at the Stanford Linear Accelerator Facility (SLAC) [6, 7].

Another crucial development in the theory of quarks and gluons was the formulation of non-Abelian gauge theories by Yang and Mills in 1954 [8], which are generalizations of the U(1) gauge theory that saw overwhelming success in describing the electromagnetic interaction. Yang-Mills theories are built on the mathematical structure of Lie groups, specifically

the special unitary group SU(N), the set of $N \times N$ unitary matrices with determinant 1. Yang-Mills theory became the best candidate for the theoretical description of partons after it was shown by Gross, Wilczek, and Politzer to be asymptotically free [9]; a necessary feature of a theory describing the interactions of partons, given the earlier discovery of Bjorken and the experiment at SLAC. Furthermore, Yang-Mills theory predicted the existence of a vector boson, identified with the gluon, needed for a complete description of hadrons in terms of partons. Finally, the SU(3) gauge specifically had the properties consistent with the additional quantum number, called color, needed to describe certain hadronic states. SU(3) gauge theory applied to the description of the quarks and gluons in the strong interaction is called quantum chromodynamics (QCD). For an overview of QCD and the SU(3) gauge group see Appendix B.

The complete theory of the strong interaction described by QCD contains six flavors of quarks, their corresponding anti-quarks, and the gluons, which can be identified with the partons in the parton model. The quarks are denoted: u, d, s, c, b, t for the up, down, strange, charm, bottom, and top quarks, respectively, and in order of increasing mass; while their corresponding anti-quarks are denoted by: $\bar{u}$, $\bar{d}$, $\bar{s}$, $\bar{c}$, $\bar{b}$, $\bar{t}$. Each (anti-)quark comes with a color charge: (anti-)red, (anti-)green, or (anti-)blue, while a gluon comes with one of eight combinations of color and anti-color, depending on the chosen SU(3) basis. Quarks also interact via electromagnetism and carry fractional electric charge, $+2/3$ for the up, charm, and top quark, and $-1/3$ for the down, strange, and bottom quark. The signs of these charges are switched in the case of anti-quarks.

Quarks and gluons combine into composite particles in colorless combinations due to the observed phenomenon of color confinement. A colorless combination can be formed by taking three (anti-)quarks of each color, (anti-)red, (anti-)green, and (anti-)blue, or by a quark anti-quark pair carrying some color and its corresponding anti-color. The simplest baryons are formed in the first of these cases, while the simplest mesons are formed in the second. Though no analytic proof of color confinement exists, it can be understood as a

result of the strength of the QCD interaction increasing at large distances, or low energy scales.

The strength of the strong interaction, or the strength at which quarks couple to gluons, is represented by the strong coupling constant, $\alpha_s(\mu)$, where μ is the energy scale. It obeys the differential equation:

$$\frac{\mathrm{d}\alpha_s/4\pi}{\mathrm{d}\ln\mu^2} = \beta\left(\alpha_s/4\pi\right) \ , \tag{1}$$

where the function β can be calculated perturbatively, by expansion in α_s, in the region where the coupling is sufficiently weak, $\alpha_s(\mu) \ll 1$. At the lowest order in α_s, the beta function is

$$\beta\left(\alpha_s/4\pi\right) = -\beta_0\frac{\alpha_s^2}{16\pi^2} + \mathcal{O}\left(\alpha_s^3\right) \ , \quad \beta_0 = \frac{11}{3}C_A - \frac{4}{3}T_F n_f \ , \tag{2}$$

where n_f is the number of quark flavors under consideration, $C_A = 3$ and $T_F = 1/2$ in QCD. In this dissertation, n_f is taken to equal 6, the total number of quark flavors in QCD; however, there are other approaches to calculations in which heavy quarks are taken to effectively decouple from the theory, leading to the consideration of a smaller number of quark flavors. For example, if the top quark is decoupled, then $n_f = 5$, which would be useful at energy scales at which $\mu \ll m_t$, m_t being the top quark mass. Using Eq. (2) to solve Eq. (1), leads to

$$\frac{\alpha_s}{4\pi} = \frac{1}{\beta_0\ln\left(\mu^2/\Lambda^2_{\mathrm{QCD}}\right)} + \dots \ , \tag{3}$$

where it can be seen that the coupling becomes vanishingly small as $\mu \to \infty$, which is exactly the property of asymptotic freedom discovered by Gross, Wilczek, and Politzer. Λ_{QCD} is defined to be the scale at which the coupling formally approaches infinity, and therefore the perturbative calculation of α_s, and perturbative QCD in general, is only valid at scales

$\mu \gg \Lambda_{\rm QCD}$.

Parton distributions carry information about the low energy behavior of partons and, based on the strength of the coupling at low energy scales, are not calculable in perturbation theory. However, the direct measurement of PDFs from experimental data is made possible through factorization, where the short-distance behavior associated with high-energy scattering can be systematically separated from the long-distance behavior of partons. Because PDFs exhibit the property of universality, the PDF data associated with a hadron in one experiment, can then be used in predicting the results of another experiment involving the same kind of hadron. The universality of PDFs allow experimentalists to test for the validity of PDF data, making them useful objects in the description of hadron structure.

In 1974, Wilson proposed a method of performing field theory calculations in a fundamentally nonperturbative way called lattice gauge theory [10], and in the specific case of quantum chromodynamics, lattice QCD (LQCD). In Wilson's approach, calculations are performed on a discretized, four dimensional, Euclidean spacetime; in contrast to the Minkowskian spacetime on which QCD resides. The complexity of such calculations demands the use of computational methods, and therefore the usefulness of the LQCD approach has increased with that of computational power.

Because LQCD provides a method for the calculation of nonperturbative objects, the extraction of PDFs from LQCD calculations has gained a considerable amount of attention and support within the last decade. In addition to the usual parton distributions that are obtained from experiment, lattice methods also show promise for the extraction of distributions that cannot be obtained from experimental methods. In other words, lattice calculations offer the opportunity for physicists to gain new insight into hadron structure and the fundamental processes described by QCD. The process of relating lattice results to "physical" PDFs, however, is a nontrivial process that has motivated the development of new calculational techniques.

PDFs are defined on the lightcone in Minkowski space, and so the Euclidean nature of

lattice methods creates a barrier to the direct calculation of matrix elements with lightlike separation; historically, this has lead to the indirect method of calculating the moments of PDFs described by local operators. New methods, however, allow for the direct extraction of distributions from lattice results. Namely, the method of quasidistributions developed by Xiangdong Ji [11], and that of pseudodistributions developed by Anatoly Radyushkin [12]. Both of these methods are motivated by the groundbreaking proposal by Ji to calculate the matrix elements of bilocal operators at spacelike separations. The quasidistribution method involves a large momentum factorization, while that of pseudodistributions involves a short distance factorization, which leads, in both cases, to a perturbatively calculable matching relation, from which one can obtain the lightcone PDF.

The derivation of the matching relations for the pseudodistribution method applied to the extraction of gluon PDFs is the motivation for the coordinate-space calculations outlined in this dissertation. Performing these calculations at the operator level provides a general process independent result, allowing for the application of the resulting operator to distributions other than the basic PDFs discussed in this text.

In Chapter 2, the parton model in introduced in the context of deeply inelastic scattering (DIS), along with facorization theorems for extracting PDFs from the DIS structure functions.

An overview of the twist-2 PDFs and their operator definition is given in Chapter 3. Then, the pseudistribution method is detailed for the case of quark distributions.

Chapter 4 outlines the methods used in the calculation: the background field method and the heat-kernel expansion [13, 14], which allow for the direct calculation of the gluon bilocal operator in an explicitly gauge invariant form.

The results for operators with open index are given in Chapter 5, along with a discussion of the various multiplicatively renormalizable quantities at spacelike separations. Namely, the somewhat nontrivial ultraviolet (UV) contributions of the vertex term are discussed.

The specific cases of the unpolarized and polarized forward matrix element are detailed

in Chapter 6, including an analysis of their Lorentz decompositions. This provides a natural connection between the spacelike distribution, and the distribution constructed from the twist-2 gluon operator at lightlike separation. Matching conditions connecting lattice data to polarized and unpolarized gluon lightcone distributions are detailed and discussed. Finally, we briefly describe the uses of our results in completed and ongoing lattice extractions of gluon PDFs.

CHAPTER 2
THE PARTON MODEL

Parton distribution functions are the fundamental objects to be determined in the investigation of hadron structure, and the most basic of these, quark PDFs, come in three different types: unpolarized, helicity, and transversity. Unpolarized PDFs carry information about the longitudinal momentum fraction carried by a parton, while helicity PDFs carry information about the momentum fraction of partons with polarization parallel or antiparallel to that of a longitudinally polarized hadron, and transversity PDFs carry information about the momentum fraction of a parton with polarization parallel or antiparallel to that of a transversely polarized hadron. Fig. 1 gives a schematic representation of each kind of PDF.

In addition to the basic PDF, there are a number of generalized PDFs that contain additional information about the behavior of matter inside hadrons. These generalized functions include distribution amplitudes (DAs), generalized parton distributions (GPDs), and transverse momentum dependent distributions (TMDs).

Of central importance to the extraction of PDFs is deeply inelastic scattering (DIS), a high energy process in which a lepton (typically an electron) probes the internal structure of some hadron. As a consequence, the hadron fragments into a number of outgoing composite particles, and the fermion undergoes a change in energy and momentum. The simplest of these processes, simply called DIS, is fully inclusive, meaning that the final state products of the interaction are averaged over, and only the scattering angle θ, and the lepton's outgoing energy E' are measured. More complicated inelastic processes exist, such as semi-inclusive DIS (SIDIS), and deeply virtual Compton scattering (DVCS), which are primarily used in the extracted of TMDs, and GPDs, respectively.

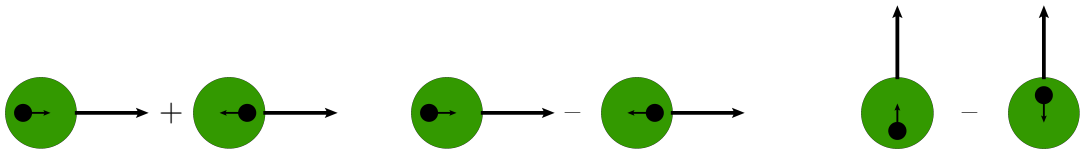

$f_i(x) = f^{\uparrow}(x) + f^{\downarrow}(x)$ $\Delta f_i(x) = f^{\uparrow}(x) - f^{\downarrow}(x)$ $\delta f_i(x) = f_{\perp}^{\uparrow}(x) + f_{\perp}^{\downarrow}(x)$

(a) (b) (c)

FIG. 1: Schematic illustration of PDFs. Direction of motion is left to right in each diagram. (a) The unpolarized PDF is the sum of partons with helicity parallel and antiparallel to that of the hadron, (b) the helicity PDF is the difference between partons with parallel and antiparallel helicity, and (c) the transversity PDF is the difference between partons with spin parallel and antiparallel to a transversely polarized hadron.

2.1 Deeply inelastic scattering

In the case of electron-proton scattering, the DIS reaction is written: $ep \to eX$, where e is the probing electron, p is the proton, and X is the sum of all hadronic final states. At leading order in quantum electrodynamics (QED), the incoming electron interacts with the proton via the exchange of a virtual photon (assuming here that weak interactions can be neglected). Diagrammatically, DIS can be represented by Fig. 2(a). The kinematic equation for DIS is written:

$$\ell + p = \ell' + p_X \ , \tag{4}$$

where ℓ/ℓ' are the initial/final state electron momentum, p is the proton momentum, and p_X is the total momentum of the final state remnants. The momentum transfer in the DIS case can be written as: $q = \ell - \ell'$, which at leading order is just the momentum of the

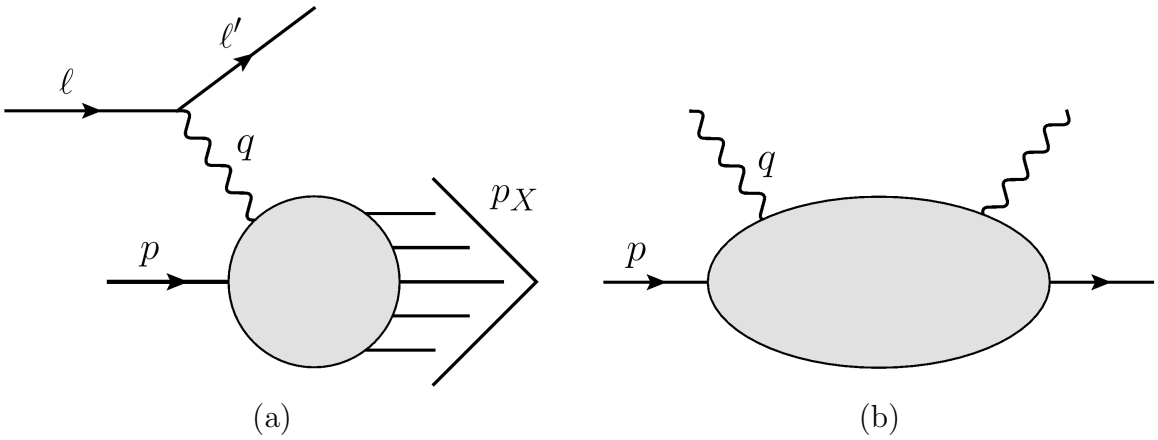

FIG. 2: Diagrammatic representation of (a) DIS at leading order in QED, and (b) the hadronic tensor.

exchanged virtual photon. Because q is a spacelike four-vector $q^2 < 0$, it is useful to define the positive-definite quantity $Q = \sqrt{-q^2}$.

Rearranging Eq. (4) and then squaring leads to the following equation in terms of Lorentz invariants:

$$m_X^2 = m^2 + 2(qp) - Q^2 \ , \tag{5}$$

where m is the proton mass, and m_X is the mass of the final states. The notation (qp) denotes the contraction of two four-vectors. In the kinematical region where $Q^2, m_X^2 \gg m^2 \sim \Lambda_{\rm QCD}$, lepton and quark masses can be neglected. It is convenient to define the Bjorken-x variable:

$$x = \frac{Q^2}{2(qp)} \ , \tag{6}$$

which takes physical values between 0 and 1.

Again, working at leading order in QED, the DIS scattering cross section can be written

in the Lorentz invariant form:

$$E'\frac{\mathrm{d}\sigma}{\mathrm{d}^3\boldsymbol{\ell}'} \simeq \frac{8\pi^3\alpha^2}{s}\sum_X \delta^{(4)}\left(p_X - p - q\right)\left|\left\langle \ell'\right| j^e_\xi \left|\ell\right\rangle \frac{1}{q^2}\left\langle X\right| j^\xi \left|p\right\rangle\right|^2$$
$$= \frac{2\alpha^2}{sQ^4} L_{\mu\nu}W^{\mu\nu} \ , \tag{7}$$

where $s = (\ell + p)^2$ is the squared center-of-mass energy.

The second line of Eq. (7) is written in terms of the leptonic $L_{\mu\nu}$, and hadronic $W^{\mu\nu}$ tensors. The leptonic tensor at leading order is simply the result for tree level Compton scattering. Assuming an unpolarized electron, and that the electron mass can be neglected, this is:

$$L_{\mu\nu} \simeq \frac{1}{2}\,\mathrm{Tr}\,\boldsymbol{\ell}\gamma_\mu\boldsymbol{\ell}'\gamma_\nu = 2\left(\ell_\mu\ell'_\nu + \ell_\nu\ell'_\mu - g_{\mu\nu}(\ell\ell')\right) \ . \tag{8}$$

Here, the 'slashed' notation is used to mean $\boldsymbol{\ell} = \gamma_\eta\ell^\eta$, and γ_η is a Dirac matrix. The hadronic tensor is:

$$W^{\mu\nu}(q,p) \equiv 4\pi^3\sum_X \delta^{(4)}\left(p_X - p - q\right)\left\langle p,s\right| j^\mu(0)\left|X\right\rangle\left\langle X\right| j^\nu(0)\left|p,s\right\rangle \ . \tag{9}$$

The hadron spin vector S is defined, as usual for a spin-$\frac{1}{2}$ target, such that $(sp) = 0$, and its normalization is taken to be $s^2 = -M^2$. Applying a spacetime translation, one of the hadronic currents can be transformed to:

$$\left\langle p,s\right| j^\mu(0)\left|X\right\rangle = \left\langle p,s\right| e^{-ipz} j^\mu(z) e^{ip_X z}\left|X\right\rangle = e^{-i(p-p_x)z}\left\langle p,s\right| j^\mu(z)\left|X\right\rangle \ . \tag{10}$$

Then, using the Fourier representation of the delta function:

$$(2\pi)^4\delta^{(4)}\left(p_X - p - q\right) = \int \mathrm{d}^4 z\, e^{-i(p_x - p - q)z} \ , \tag{11}$$

and a sum and integral over the complete set of hadronic final states:

$$\sum_X |X\rangle \langle X| = I \ , \tag{12}$$

Eq. (9) can be rewritten as:

$$W^{\mu\nu}(q,p) \equiv \frac{1}{4\pi} \int \mathrm{d}^4 z \, e^{iqz} \langle p,s| \, j^\mu(z) j^\nu(0) \, |p,s\rangle \ . \tag{13}$$

Hence, the hadronic tensor is the Fourier transform of the coordinate-space hadronic current-current correlator, where causality demands that $z^2 \geq 0$.

At large Q^2 the leading behavior of the hadronic tensor occurs near the lightcone. This is best seen by working in a reference frame where the momentum of the virtual photon in the DIS reaction points along the negative z-axis:

$$q^\mu = \left(\frac{Q^2}{2mx}, 0, 0, -\frac{Q^2}{2mx} \sqrt{1 + 4m^2x^2/Q^2} \right) \ . \tag{14}$$

At large Q^2, the lightcone components (see Appendix A) of q can be approximated as

$$q^+ = -mx \ , \qquad q^- = \frac{Q^2}{mx} \ , \tag{15}$$

and the hadronic tensor then takes the form:

$$W^{\mu\nu}(q,p) \equiv \frac{1}{4\pi} \int \mathrm{d}z^+ e^{iQ^2 z^+/mx} \int \mathrm{d}z^- \, e^{imxz^-} \int \mathrm{d}^2 z_\perp \, \langle p,s| \, j^\mu(z) j^\nu(0) \, |p,s\rangle \ . \tag{16}$$

Because of the oscillatory behavior of the exponential in Eq. (16), the integral will vanish unless the matrix element is dominated by the region in z where

$$z^+ \sim \frac{mx}{Q^2} \ , \qquad z^- \sim \frac{1}{mx} \ . \tag{17}$$

Therefore, assuming that the matrix element is smooth on the scale of $1/Q$, the integral, and subsequently the DIS process, is dominated by the region of z close to the lightcone, $z^2 \approx 0$.

Electromagnetic current conservation $q_\mu W^{\mu\nu} = 0$, hermiticity $(W^{\mu\nu})^* = W^{\nu\mu}$, linearity in S, and the parity invariance of the strong interaction put constraints on the hadronic tensor. Accounting for these properties, the Lorentz decomposition of $W^{\mu\nu}$ is:

$$W^{\mu\nu} = \left(-g^{\mu\nu} + \frac{q^\mu q^\nu}{q^2}\right) F_1\left(x, Q^2\right) + \frac{(p^\mu - q^\mu(qp)/q^2)(p^\nu - q^\nu(qp)/q^2)}{(qp)} F_2\left(x, Q^2\right)$$
$$+ i\epsilon^{\mu\nu\alpha\beta}\frac{q_\alpha s_\beta}{(qp)} g_1\left(x, Q^2\right) + i\epsilon^{\mu\nu\alpha\beta}\frac{q_\alpha\left(s_\beta - p_\beta\frac{(qs)}{(qp)}\right)}{(qp)} g_2\left(x, Q^2\right) \ , \tag{18}$$

where the Levi-Civita tensor $\epsilon^{\mu\nu\alpha\beta}$ is defined such that $\epsilon^{0123} = -1$. The functions F_1, F_2, g_1, and g_2, called structure functions, are functions of the Lorentz invariant quantities, x and Q^2.

In the case of an unpolarized hadron, the contributions from g_1 and g_2 are zero, and the differential cross section can be written:

$$\frac{\mathrm{d}^2\sigma}{\mathrm{d}x\mathrm{d}y} \simeq \frac{4\pi\alpha^2}{xyQ^2}\left[\left(1 - y - \frac{x^2y^2M^2}{Q^2}\right) F_2\left(x, Q^2\right) + y^2 x F_1\left(x, Q^2\right)\right] \ , \tag{19}$$

where y is defined as:

$$y = \frac{(qp)}{(\ell p)} \ . \tag{20}$$

2.2 Parton model

Before discussing QCD, the DIS cross section can be related to the early parton model of Feynman, Bjorken, and Paschos, namely that

$$\mathrm{d}\sigma = \sum_j \int_x^1 \mathrm{d}\xi \mathrm{d}\sigma_j^{\mathrm{p}} f_j(\xi) \ , \tag{21}$$

where the sum is over parton flavors. The RHS of Eq. (21) is a factorization that ignores the contributions from strong interaction dynamics, where $\mathrm{d}\sigma_j^p$ is the partonic level cross section, i.e. the high energy or hard scattering of a lepton with quark j, and the function f_j is the PDF for that same quark. The variable ξ is defined in terms of lightcone coordinates as $\xi = k^+/p^+$, the fraction of the quark's plus momentum to that of the hadron. A boost invariant quantity, ξ is a natural parameter to work with that can be defined in any reference frame.

The limits on the momentum fraction $x \leq \xi \leq 1$ are controlled by kinematical restrictions on the DIS process: positivity of the final state energy, $p^+ - \xi p^+ \geq 0$, and positivity of the energy in the hard scattering, $q^+ + \xi p^+ \geq 0$. The second constraint can be rewritten in terms of Bjorkan-x by multiplying through q^-, leading to $\xi \geq Q^2/2(pq)$.

At the level of the hadronic tensor, the parton model gives:

$$W^{\mu\nu} = \sum_j \int \frac{\mathrm{d}\xi}{\xi} C^{\mu\nu}_{j,\mathrm{p}} f_j(\xi) \ , \tag{22}$$

where the $1/\xi$ term comes from the fact that the center-of-mass energy at the parton level $(\ell + \xi p)^2 \simeq 2\xi(\ell p) \simeq \xi s$. The partonic tensor, $C^{\mu\nu}_{j,\mathrm{p}}$, is just Eq. (13), but with the hadron states replaced with parton ones. In the case of a spin-$\frac{1}{2}$ quark of type j and momentum $k^\mu = (k^+, 0, 0, 0)$, it reads:

$$C^{\mu\nu}_{j,\mathrm{p}} = e_j^2 \left(2k^\mu k^\nu + q^\mu k^\nu + q^\nu k^\mu - g^{\mu\nu}(kq)\right) \frac{x}{Q^2} \delta(\xi - x) \ , \tag{23}$$

e_j being the fraction charge of the quark under consideration. The reason for the definition of x is now clear, since the parton momentum fraction is exactly equal to x in the parton model. Combining Eqs. (18), (22), and (23), the structure functions can be written in terms

of the PDFs:

$$F_2\left(x,Q^2\right)=\sum_j e_j^2 x f_j(x)\ ,\quad F_1\left(x,Q^2\right)=\frac{1}{2}\sum_j e_j^2 f_j(x)=\frac{1}{2x}F_2\left(x,Q^2\right)\ . \tag{24}$$

The RHS of F_1 and F_2 are both independent of Q^2 at fixed x, which is exactly the prediction of Bjorken scaling. Of course, everything done here neglects the contribution from QCD, and formally only holds exactly in the limit $Q^2\to\infty$. Nevertheless, the approximate Bjorken-scaling has been confirmed over a wide range of Q^2 and x (see Fig. 3).

2.3 QCD corrections

The F_1, F_2, and g_1 structure functions can be generalized to include higher order corrections in QCD (the g_2 structure function is power suppressed in DIS by at least $\mathcal{O}(m/Q)$):

$$F_1^{Vh}(x,Q^2)=\sum_i\int_x^1\frac{\mathrm{d}\xi}{\xi}\,\widehat{F}_{1i}^V\left(\frac{x}{\xi},\frac{Q^2}{\mu^2},\frac{\mu_f^2}{\mu^2},\alpha_s\right)f_{i/h}\left(\xi,\mu_f^2,\mu^2\right)+\mathcal{O}\left(\frac{m^2}{Q^2},\frac{\Lambda_{\mathrm{QCD}}^2}{Q^2}\right)\ , \tag{25}$$

$$F_2^{Vh}(x,Q^2)=\sum_i\int_x^1\mathrm{d}\xi\,\widehat{F}_{2i}^V\left(\frac{x}{\xi},\frac{Q^2}{\mu^2},\frac{\mu_f^2}{\mu^2},\alpha_s\right)f_{i/h}\left(\xi,\mu_f^2,\mu^2\right)+\mathcal{O}\left(\frac{m^2}{Q^2},\frac{\Lambda_{\mathrm{QCD}}^2}{Q^2}\right)\ , \tag{26}$$

$$g_1^{Vh}(x,Q^2)=\sum_i\int_x^1\frac{\mathrm{d}\xi}{\xi}\,\widehat{g}_{1i}^V\left(\frac{x}{\xi},\frac{Q^2}{\mu^2},\frac{\mu_f^2}{\mu^2},\alpha_s\right)\Delta f_{i/h}\left(\xi,\mu_f^2,\mu^2\right)+\mathcal{O}\left(\frac{m^2}{Q^2},\frac{\Lambda_{\mathrm{QCD}}^2}{Q^2}\right)\ , \tag{27}$$

where $\widehat{F}_{1i}^V$, $\widehat{F}_{2i}^V$, and $\widehat{g}_{1i}^V$ are coefficient functions that can be calculated perturbatively to some order in α_s, and the scale dependence of $\alpha_s(\mu^2)$ has been suppressed. The index i runs over all quarks, antiquarks, and gluons, while the electroweak boson being exchanged in the DIS process is represented by V, and the hadron under investigation by h.

As mentioned earlier, one of the important properties of PDFs is universality, where the PDF for some parton in a hadron is independent of the scattering process. This means, for example, that a PDF extracted from a DIS experiment, could be used to make predictions about a Drell-Yan interaction (hadron-hadron collision). Universality is what makes PDFs a meaningful object in the description of hadron structure.

In contrast to the PDFs, the coefficient functions are dependent on the specifics of the scattering process under consideration, namely the vector boson, V, and the parton, i. However, they are independent of the specific hadron, as they are completely independent of long-distance effects. It is exactly these properties that allow the coefficient functions to be calculated in perturbation theory.

There are two scales associated with the PDFs and coefficient functions: the usual renormalization scale, μ, necessary in any QCD calculation, and the factorization scale, μ_f, specific to factorization, and associated with separating the long and short distance behavior. In calculating the coefficient functions, the scale dependence appears in logarithms such as $\ln\left(Q^2/\mu^2\right)$, whose size can be controlled by setting $\mu = Q$. Oftentimes the factorization scale will also be set equal to the renormalization scale $\mu = \mu_f$, but this isn't always a convenient choice. Either way, the value of both scales can be chosen freely, since the physical observable structure functions are independent of both.

As discussed before, at large Q^2 and constant x the leading behavior in the hadronic tensor, and therefore in the structure functions, is near the lightcone. Each structure function then has power suppressed corrections of order m^2/Q^2 and $\Lambda^2_{\rm QCD}/Q^2$, a crucial feature of QCD factorization. As will be shown, this leading behavior is associated with what are called twist-2 operators, and for this reason the PDFs under investigation here are called twist-2 PDFs.

The scale dependence of the PDFs above hints at the fact that they have their own renormalization group equations. The renormalized unpolarized PDF can be written:

$$f_{i/h}\left(\xi,\mu^2\right) = \sum_{i'}\int_\xi^1 \frac{{\rm d}\xi'}{\xi'} Z_{ii'}\left(\xi',\alpha_s(\mu^2)\right) f_{(0)i'/h}\left(\xi'/\xi\right) \ , \tag{28}$$

where $f_{(0)i'/h}$ is the bare, or unrenormalized, PDF, and $Z_{ii'}$ is the renormalization kernal. Taking the derivative of Eq. (28) with respect to $\ln\mu^2$, and utilizing the scale independence of the bare PDF leads to the Dokshitzer-Gribov-Lipatov-Altarelli-Parisi (DGLAP) [16–18]

evolution equation:

$$\frac{\mathrm{d}}{\mathrm{d}\ln\mu^2} f_{i/h}\left(\xi,\mu^2\right) = \sum_{i'} \int_\xi^1 \frac{\mathrm{d}\xi'}{\xi'} P_{ii'}\left(\xi',\alpha_s(\mu^2)\right) f_{i'/h}\left(\xi'/\xi,\mu^2\right) \ , \tag{29}$$

where the evolution kernel $P_{ii'}$ is perturbatively calculable, as it corresponds with the UV behavior of the bare PDF. The evolution kernel is defined by:

$$\frac{\mathrm{d}}{\mathrm{d}\ln\mu^2} Z_{ii'}\left(\xi,\alpha_s(\mu^2)\right) = \sum_{j} \int_\xi^1 \frac{\mathrm{d}\xi'}{\xi'} P_{ij}\left(\xi',\alpha_s(\mu^2)\right) Z_{ji'}\left(\xi/\xi',\alpha_s(\mu^2)\right) \ . \tag{30}$$

Similar equations can be written for the helicity PDFs.

Calculation of the coefficient functions is accomplished order by order in perturbation theory. First, the parton level structure functions and PDFs are calculated. Then, the coefficient functions can be extracted, since they are independent of long-distance physics and so will be the same at the parton or hadron level. At leading order, the values of the coefficient functions must reproduce the parton model results in Eq. (24). Calculating past the leading order requires a definition of the PDF in QCD.

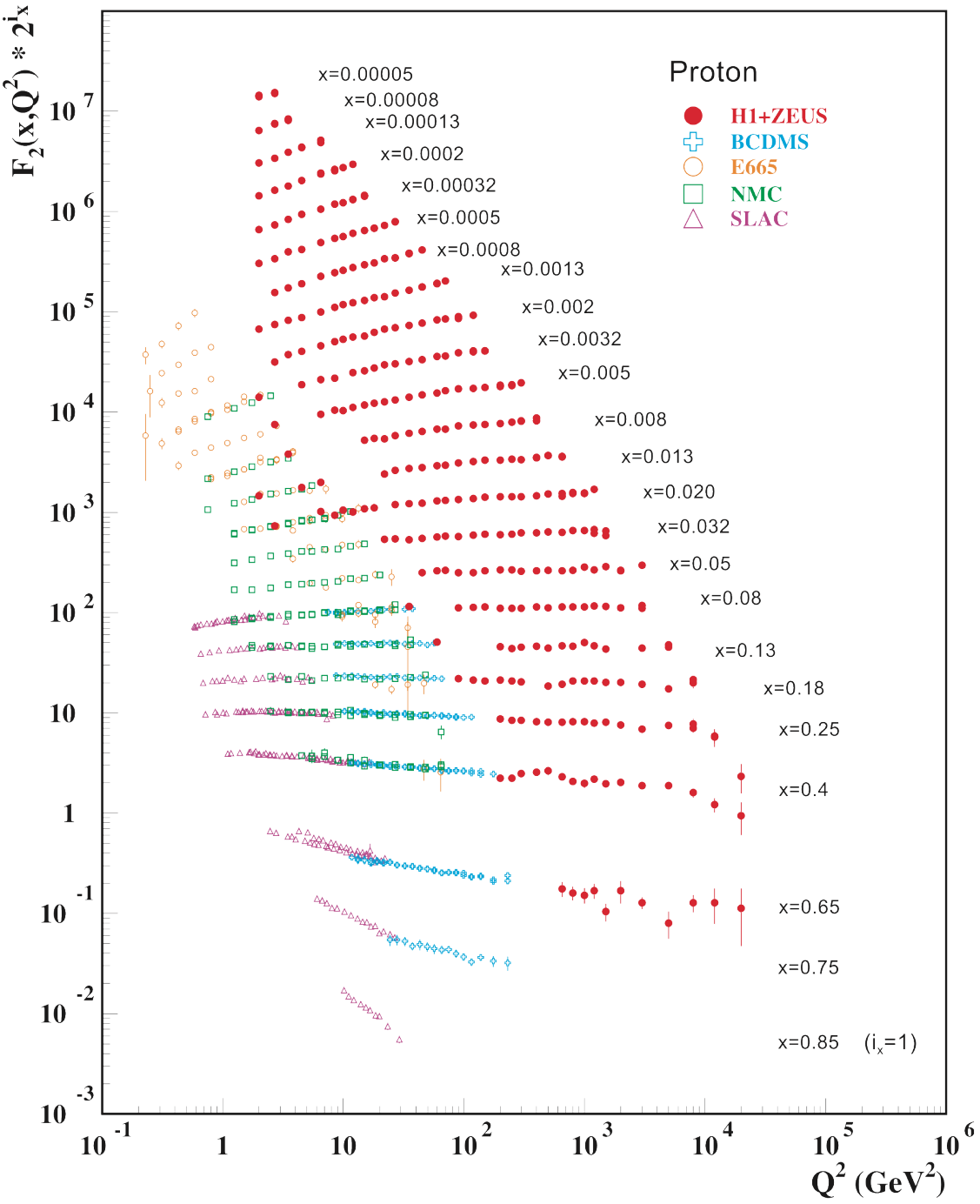

FIG. 3: Unpolarized proton structure function F_2 data compiled by the Particle Data Group. For the sake of comprehension, F_2 is multiplied by 2^{i_x}, where i_x is the number of the x bin, ranging from $i_x = 1$ ($x = 0.85$) to $i_x = 24$ ($x = 0.00005$). [15]

CHAPTER 3

PARTON DISTRIBUTION FUNCTIONS

By taking advantage of the properties of QCD interactions, Eq. (29) can be rewritten in a simpler form. Because quark-gluon interactions are independent of quark flavor, the evolution kernels for quarks can be rewritten as $P_{q^i q^j} = \delta_{q^i q^j} P$, and furthermore in the case where quark masses are neglected, the mixing kernels can be simplified to $P_{g q^i} = P_{gq}$, and $P_{q^i g} = P_{qg}$, accounting for the fact that interaction with a specific flavor of quark happens with equal probability for massless quarks. Additionally, the evolution equations can be written in terms of the quark singlet distribution:

$$f_S(\xi) = \sum_i^{2n_f} f_i(\xi) \ , \tag{31}$$

where n_f is the number of quark flavors, and i is a sum over quark and anti-quarks. The subscript h is suppressed here, with the understanding that the PDF properties under investigation can be applied to a general hadronic state. The resulting evolution equations are then:

$$\frac{\mathrm{d}}{\mathrm{d}\ln\mu^2} f_S\left(\xi,\mu^2\right) = \int_\xi^1 \frac{\mathrm{d}\xi'}{\xi'}\left[P_{qq}\left(\xi',\alpha_s(\mu^2)\right) f_S\left(\xi'/\xi,\mu^2\right) + 2n_f P_{qg}\left(\xi',\alpha_s(\mu^2)\right) f_g\left(\xi'/\xi,\mu^2\right)\right] , \tag{32}$$

$$\frac{\mathrm{d}}{\mathrm{d}\ln\mu^2} f_g\left(\xi,\mu^2\right) = \int_\xi^1 \frac{\mathrm{d}\xi'}{\xi'}\left[P_{gg}\left(\xi',\alpha_s(\mu^2)\right) f_g\left(\xi'/\xi,\mu^2\right) + P_{gq}\left(\xi',\alpha_s(\mu^2)\right) f_S\left(\xi'/\xi,\mu^2\right)\right] , \tag{33}$$

with analogous equations for the helicity distributions: Δf_S and Δg. In the case of transversity distributions there are no mixing terms due to helicity conservation, and the evolution equations are diagonal in the case of a quark or gluon.

Again, being related to the PDF renormalization constants, the AP kernels can be calculated perturbatively, and at leading order in QCD they are:

Unpolarized:

$$\frac{\alpha_s}{2\pi}C_F P_{qq}^{(0)}(\xi) = \frac{\alpha_s}{2\pi}C_F\left[\frac{1+\xi^2}{1-\xi}\right]_{+(1)}, \tag{34}$$

$$\frac{\alpha_s}{2\pi}T_F P_{qg}^{(0)}(\xi) = \frac{\alpha_s}{2\pi}T_F\left(\xi^2+(1-\xi)^2\right), \tag{35}$$

$$\frac{\alpha_s}{2\pi}C_F P_{gq}^{(0)}(\xi) = \frac{\alpha_s}{2\pi}C_F\frac{1+(1-\xi)^2}{\xi}, \tag{36}$$

$$\frac{\alpha_s}{2\pi}C_A P_{gg}^{(0)}(\xi) = \frac{\alpha_s}{2\pi}2C_A\left\{\frac{\xi}{(1-\xi)_{+(1)}}+(1-\xi)\left(\frac{1}{\xi}+\xi\right)+\left(\frac{\beta_0}{4C_A}-\frac{1}{3}\frac{T_F}{C_A}\right)\delta(\xi-1)\right\}, \tag{37}$$

Helicity:

$$\frac{\alpha_s}{2\pi}C_F \Delta P_{qq}^{(0)}(\xi) = \frac{\alpha_s}{2\pi}C_F\left[\frac{1+\xi^2}{1-\xi}\right]_{+(1)}, \tag{38}$$

$$\frac{\alpha_s}{2\pi}T_F \Delta P_{qg}^{(0)}(\xi) = \frac{\alpha_s}{2\pi}T_F\left(\xi^2-(1-\xi)^2\right), \tag{39}$$

$$\frac{\alpha_s}{2\pi}C_F \Delta P_{gq}^{(0)}(\xi) = \frac{\alpha_s}{2\pi}C_F\frac{1-(1-\xi)^2}{\xi}, \tag{40}$$

$$\frac{\alpha_s}{2\pi}C_A \Delta P_{gg}^{(0)}(\xi) = \frac{\alpha_s}{2\pi}2C_A\left[\frac{\xi}{(1-\xi)_{+(1)}}+2(1-\xi)+\left(\frac{\beta_0}{4C_A}-\frac{1}{3}\frac{T_F}{C_A}\right)\delta(\xi-1)\right], \tag{41}$$

Transversity:

$$\frac{\alpha_s}{2\pi}C_F \delta P_{qq}^{(0)}(\xi) = \frac{\alpha_s}{2\pi}C_F\left\{\left[\frac{1+\xi^2}{1-\xi}\right]_{+(1)}-(1-\xi)\right\}, \tag{42}$$

$$\frac{\alpha_s}{2\pi}C_A \delta P_{gg}^{(0)}(\xi) = \frac{\alpha_s}{2\pi}2C_A\left\{\frac{\xi}{(1-\xi)_{+(1)}}+\left(\frac{\beta_0}{4C_A}-\frac{1}{3}\frac{T_F}{C_A}\right)\delta(\xi-1)\right\}, \tag{43}$$

where the plus-prescription is defined as:

$$\int_0^1 \mathrm{d}u\left[f(u)\right]_{+(a)} g(u) = \int_0^1 \mathrm{d}u f(u)\left[g(u)-g(a)\right]. \tag{44}$$

3.1 Operator definitions

The dominant distributions that are extracted from hard scattering processes are those given by the lowest twist operators, where "geometric" twist is a classification given to local operators defined as $\tau = d - s$, the dimension of the operator minus its Lorentz spin. Therefore, the leading twist operator will have minimal dimension and maximal spin, which turns out to be the case where $\tau = 2$. The leading twist PDFs can then be defined on the lightcone in terms of an expansion in local twist-2 operators.

3.1.1 Quark PDFs

In the quark case the relevant twist-2 operators can be defined for general dimension and spin as:

$$\mathcal{Q}_{\rm tw2}^{\mu_1\dots\mu_n}(0) = \bar{\psi}(z)\Gamma^{\mu_1}\overleftarrow{D}^{(\mu_2}\dots\overleftarrow{D}^{\mu_n)}\psi(0)\Big|_{z=0} , \tag{45}$$

where $(\mu_1 \dots \mu_n)$ indicates symmetrization of the Lorentz indices, and Γ^μ represents one of three relevant Dirac structures: γ^μ, $\gamma^\mu\gamma_5$, and $\gamma^\mu\gamma_5\gamma^i$, where i represents a transverse component. The covariant derivative in this case is defined as:

$$\overleftarrow{D}_\mu = \overleftarrow{\partial}_\mu - igA_\mu , \tag{46}$$

where the arrows indicate the direction in which the derivative is applied.

Using Eq. (45), the lightcone bilocal twist-2 quark operator can be defined by the Taylor series:

$$\bar{\psi}_q(z^-)\Gamma^+[z^-,0]_F\,\psi_q(0) = \sum_{n=1}^{\infty}\frac{(z^-)^n}{n!}\mathcal{Q}_{\rm tw2}^{+\dots+}(0) , \tag{47}$$

where

$$[z^-,0]_F = \mathcal{P}\exp\left[ig\int_0^{z^-}\mathrm{d}y^- t^a A_a^+\left(y^-\right)\right] \tag{48}$$

is the gauge link in the fundamental representation, with t^a the generating matrices of the SU(3) gauge group, normalized to $\mathrm{Tr}\, t^a t^b = \frac{1}{2}\delta^{ab}$.

Placing Eq. (47) into a hadronic matrix element and taking the Fourier transform, the quark PDFs can be defined as:

$$f_q(x) = \frac{1}{2}\int_{-\infty}^{\infty}\frac{\mathrm{d}z^-}{2\pi}e^{-ixp^+z^-}\,\langle p|\,\bar{\psi}_q(z^-)\gamma^+[z^-,0]_F\,\psi_q(0)\,|p\rangle \tag{49}$$

$$\Delta f_q(x) = \frac{1}{2}\int_{-\infty}^{\infty}\frac{\mathrm{d}z^-}{2\pi}e^{-ixp^+z^-}\,\langle p,s|\,\bar{\psi}_q(z^-)\gamma^+\gamma_5[z^-,0]_F\,\psi_q(0)\,|p,s\rangle \tag{50}$$

$$\delta f_q(x) = \frac{1}{2}\int_{-\infty}^{\infty}\frac{\mathrm{d}z^-}{2\pi}e^{-ixp^+z^-}\,\langle p,s|\,\bar{\psi}_q(z^-)\gamma^+\gamma_5\gamma^i[z^-,0]_F\,\psi_q(0)\,|p,s\rangle\ , \tag{51}$$

where s is the hadron spin. In order of appearance these are the unpolarized, helicity, and transversity PDFs. The antiquark PDFs can be defined from the quark PDFs by the relations:

$$f_q(x) = -f_{\bar{q}}(-x)\ ,\quad \Delta f_q(x) = \Delta f_{\bar{q}}(-x)\ ,\quad \delta f_q(x) = -\delta f_{\bar{q}}(-x)\ . \tag{52}$$

3.1.2 Gluon PDFs

For the case of gluons, the twist-2 operators are defined as:

$$\mathcal{G}_{\mathrm{tw2}}^{\mu_1\ldots\mu_n}(0) = P^{ij}G^{\mu_1 i}(z)\overleftarrow{D}^{(\mu_3}\ldots\overleftarrow{D}^{\mu_n)}G^{\mu_2 j}(0)\Big|_{z=0}\ , \tag{53}$$

with summation over transverse indices i and j. The operator P^{ij} represents one of three projections on the field strength tensor indices corresponding to

$$P^{ij} = \delta^{ij} \ , \quad P^{ij}_{\rm hel} = i\epsilon^{ij} = \tfrac{i}{2}\epsilon^{+-ij} \ , \quad P^{k\ell,ij}_{\rm lin} = \tfrac{1}{2}\delta^{ki}\delta^{\ell j} + \tfrac{1}{2}\delta^{kj}\delta^{\ell i} - \tfrac{1}{2}\delta^{k\ell}\delta^{ij} \ , \tag{54}$$

where k and ℓ represent transverse components: $\{k,\ell\} = \{1,2\}$, or $\{2,1\}$. Using Eq. (53), the ligthcone bilocal twist-2 gluon operator is defined by the Taylor series:

$$G^{+i}(z^-)[z^-,0]_A\, G^{+i}(0) = \sum_{n=1}^{\infty} \frac{(z^-)^n}{n!} \mathcal{G}^{+\ldots+}_{\rm tw2}(0) \ , \tag{55}$$

where

$$[z^-,0]_A = \mathcal{P} \exp\left[ig \int_0^{z^-} {\rm d}y^- T^a A^+_a(y^-) \right] \tag{56}$$

is the gauge link in the adjoint representation, with ${\rm Tr}\, T^a T^b = C_A \delta^{ab}$ and $C_A = 3$ in QCD.

Similarly to the quark case, the gluon PDFs can be defined as:

$$f_g(x) = \frac{1}{xp^+} \int_{-\infty}^{\infty} \frac{{\rm d}z^-}{2\pi} e^{-ixp^+z^-} \langle p|\, G^{+i}(z^-)[z^-,0]_A\, G^{+i}(0)\, |p\rangle \tag{57}$$

$$\Delta g(x) = \frac{1}{xp^+} \int_{-\infty}^{\infty} \frac{{\rm d}z^-}{2\pi} e^{-ixp^+z^-} P^{ij}_{\rm hel} \langle p,s|\, G^{+i}(z^-)[z^-,0]_A\, G^{+j}(0)\, |p,s\rangle \tag{58}$$

$$\delta g(x) = \frac{1}{xp^+} \int_{-\infty}^{\infty} \frac{{\rm d}z^-}{2\pi} e^{-ixp^+z^-} P^{k\ell,ij}_{\rm lin} \langle p,s|\, G^{+i}(z^-)[z^-,0]_A\, G^{+j}(0)\, |p,s\rangle \ , \tag{59}$$

where again the three cases, in order of appearance, are unpolarized, helicity, and transvsersity PDFs. In the case of the helicity PDF, the operator can also be written in terms of the dual gluon field:

$$P^{ij}_{\rm hel} G^{+i}(z^-)[z^-,0]_A\, G^{+j}(0) = G^{+i}(z^-)[z^-,0]_A\, \widetilde{G}^{+i}(0) \ , \tag{60}$$

with $\widetilde{G}^{\mu\nu} = \frac{1}{2}\epsilon^{\mu\nu\xi\eta} G_{\xi\eta}$ being the dual gluon field strength tensor. Because the gluon is its

own antiparticle, the gluon distributions have the properties:

$$f_g(x) = -f_g(-x) \ , \quad \Delta g(x) = \Delta g(-x) \ , \quad \delta g(x) = -\delta g(-x) \ . \tag{61}$$

3.2 Pseudodistributions

While lattice QCD provides a nonperturbative approach to QCD calculations, the direct extraction of PDFs is not possible since they are fundamentally defined at lightlike separations $z^2 = 0$, which is not accessible in Euclidean spacetime. An effective route has been to reconstruct the PDFs from the calculation of their moments in the Taylor expansions given in Eqs. (47) and (55). More recent approaches, however, involve the direct extraction of PDFs from the lattice, and involve the computation of matrix elements at spacelike separations $z = (0, 0, 0, z_3)$ [11]. The method central to the content of this dissertation is that of pseudodistributions [12], which is essentially a coordinate space based, short distance factorization with power suppressed corrections of order $\mathcal{O}(z_3^2 m^2, z_3^2 \Lambda_{\rm QCD}^2)$. In this section, we describe the procedure by which pseudodistributions can be used to extract twist-2 PDFs in the $\overline{\rm MS}$ renormalization scheme from lattice calculations. Specifically, the pseudodistribution method will be outlined for the unpolarized singlet quark distribution, but the methods are general and can also be applied to gluonic PDFs.

Within the pseudodistribution framework it is natural to work in terms of Ioffe-time distributions (ITDs), $\mathcal{I}(\nu)$ [19], which on the lightcone are directly related to matrix elements of bilocal operators. Therefore, they are also directly related to the PDFs, $f(x)$, and in the case of unpolarized quarks the relation is:

$$\mathcal{I}\left(\nu\right) = \int_{-1}^{1} \mathrm{d}x e^{-ix\nu} f_S\left(x\right) = \frac{1}{2}\frac{1}{p^+} \sum_f \left\langle p\right| \bar{\psi}_f(z^-)\gamma^+ \psi_f(0) \left|p\right\rangle \ , \tag{62}$$

where the Ioffe-time [20] is defined as $\nu = -(pz)$, and in the lighcone case is $\nu = -p^+ z^-$. The sum is over quark and antiquark flavors. A direct generalization of the ITD is used in

the pseudodistribution method, called the Ioffe-time pseudodistribution (pseudo-ITD). Getting the pseudo-ITD requires the Lorentz decomposition of the matrix element at arbitrary spacetime separation, defined for general Dirac matrix:

$$M^{\mu}\left(z,p\right)=\sum_{f}\left\langle p\right|\bar{\psi}_{f}(z)\gamma^{\mu}\,\psi_{f}(0)\left|p\right\rangle \ . \tag{63}$$

The Lorentz decomposition is then:

$$M^{\mu}\left(z,p\right)=2p^{\mu}\mathcal{M}_{p}\left(\nu,-z^{2}\right)+z^{\mu}\mathcal{M}_{z}\left(\nu,-z^{2}\right) \ . \tag{64}$$

Taking the + component of Eq. (64) at lightlike separations, only $\mathcal{M}_p$ survives, and can therefore be identified with the lightcone ITD. This means that, at spacelike separations, $\mathcal{M}_p$ is the pseudo-ITD, where $\mathcal{M}_z$ is associated with purely higher twist effects in the lightcone limit. Taking the index $\mu = 0$ will remove this contaminating term.

A property of pseudo-ITDs is the presence of additional UV divergences both linear and logarithmic, they are associated with the gauge link along a spacelike direction, and do not appear when taking matrix elements at lightlike separations. Taking advantage of the multiplicative renormalizability of these divergences, they can be straightforwardly removed through the ratio method [21, 22], where a reduced pseudo-ITD (pseudo-rITD) is defined as:

$$\mathfrak{M}\left(\nu,z_{3}^{2}\right)=\frac{\mathcal{M}_{p}\left(\nu,z_{3}^{2}\right)}{\mathcal{M}_{p}\left(0,z_{3}^{2}\right)} \ . \tag{65}$$

Taking the ratio of the pseudo-ITD to its rest frame value will remove the linear UV divergence, while leaving its leading twist, ν dependent, structure intact. Furthermore, as long as the pseudo-ITDs in the numerator and denominator have the same UV anomalous dimension, which may not always be the case, the logarithmic UV divergences are also completely removed in the ratio method. This leaves a renormalization group invariant (RGI) object, whose z_3 dependence at leading order exists entirely in the evolution logarithms as $\ln\left(\mu^{2}z_{3}^{2}\right)$.

Hence, the z_3^2 behavior matches the behavior of μ^2 in the $\overline{\text{MS}}$ scheme, and the pseudo-rITD admits its own approximate evolution equation at short distances. At leading order in QCD this is:

$$\frac{\mathrm{d}}{\mathrm{d}\ln z_3^2}\mathfrak{M}\left(\nu, z_3^2\right) = -\frac{\alpha_s}{2\pi}C_F\int_0^1 \mathrm{d}u P_{qq}^{(0)}(u)\mathfrak{M}\left(u\nu, z_3^2\right) + \mathcal{O}\left(z_3^2 m^2, z_3^2\Lambda_{\text{QCD}}^2\right) \ , \tag{66}$$

where $P_{qq}^{(0)}$ is the quark-quark evolution kernel defined in Eq. (34), and the quark-gluon mixing term has been neglected.

The pseudo-ITD at $\nu = 0$ will still have contributions from higher twist effects, and in principle may serve to reduce the contribution from higher twist contaminations in the pseudo-rITD.

In principle, taking the $z_3 \to 0$ limit of the pseudo-rITD while holding ν fixed produces the lightcone ITD and subsequently the twist-2 PDF. However, this is not directly possible due to the logarithmic singularities in z_3^2 related to PDF evolution. Naturally, this leads to the construction of a matching relation that connects the lattice calculable pseudo-rITD to the lightcone ITD in the $\overline{\text{MS}}$ scheme.

$$\mathfrak{M}\left(\nu, z_3^2\right) = \int_{-1}^1 \mathrm{d}u\, \mathcal{C}\left(u, z_3^2\mu^2, \alpha_s\right)\mathcal{I}\left(u\nu, \mu^2\right) + \mathcal{O}\left(z_3^2 m^2, z_3^2\Lambda_{\text{QCD}}^2\right) \ , \tag{67}$$

where at short distances the pseudo-rITD factorizes into the convolution of the matching kernel, $\mathcal{C}$, and the lightcone ITD. Again, the gluonic contribution has been neglected here, but would appear as a mixing term with a similarly peturbatively calculable matching kernel.

The specific complications that arise in defining the pseudo-ITDs in the case of gluons will be outlined in Chapter 6, along with the matching equations for the unpolarized and helicity gluon PDFs. The gluon results can also be found in the recent papers [23–25]. The quark pseudodistributions have been explored in [26–28].

CHAPTER 4

METHODS OF CALCULATION

The gluon bilocal operator was calculated using the same methods employed by Ian Balitsky and Vladimir Braun in their 1989 paper [14]. The central idea here is a coordinate space calculation using the background field method along with the Schwinger parametrization of the propagator via the QCD heat kernel. The coordinate space based approach allows for the calculation of corrections to gluon operators in an explicitly gauge invariant form, where other methods typically make computations unnecessarily complicated.

The calculation also employs the $\overline{\text{MS}}$ renormalization scheme, and thus calculations were performed in d spacetime dimensions. Furthermore, the convention in this text is $d = 4-2\epsilon_{UV}$ in the case of UV divergences, and $d = 4+2\epsilon_{IR}$ in the case of infrared (IR) divergences, such that in both cases the limit will be $\epsilon_{IR/UV} \to 0^+$. Throughout the remainder of this paper the IR scale μ_{IR} should be understood to have the exact same meaning as the factorization scale μ_R mentioned earlier.

4.1 Background field method

The idea behind the background, or external, field method is to divide the field under consideration into a "classical" background field with virtualities below some point, μ_1^2 $\left(\bar{\psi}, \psi, A\right)$, and a quantum field with virtualities above μ_1^2 $\left(\bar{\phi}, \phi, \mathcal{A}\right)$, but below some higher virtuality μ_2^2. Integrating over the quantum fields produces a result in terms of the external (or background) fields at the lower renormalization point μ_1^2. Splitting the quark and gluon fields in this way leads to a modified QCD Lagrangian:

$$\begin{aligned}\mathcal{L} = &-\frac{1}{4g^2}\left(G^a_{\mu\nu} + D_\mu \mathcal{A}^a_\nu - D_\nu \mathcal{A}^a_\mu + f^{abc}\mathcal{A}^b_\mu \mathcal{A}^c_\nu\right)^2 - \frac{1}{2g^2}\left(D^\mu \mathcal{A}^a_\mu\right)^2 \\ &+ \left(\bar{\phi} + \bar{\psi}\right)\left(i\not{D} + \mathcal{A}^a_\mu \gamma^\mu t^a\right)(\phi + \psi) + \mathcal{L}_{gh}\ . \end{aligned} \tag{68}$$

Here, the covariant derivative $D_\mu = \partial_\mu - iA_\mu$ and the field strength tensor $G^a_{\mu\nu} = D_\mu A^a_\nu - D_\nu A^a_\mu$ are defined only in terms of the background field. The background field (BF) gauge, given by:

$$\mathcal{L}_{\rm GF} = -\frac{1}{2g^2}\left(D^\mu \mathcal{A}^a_\mu\right)^2 \ , \tag{69}$$

is applied to the quantum fields, and is analogous to the Feynman-'t Hooft gauge at lowest order in the external field expansion. In order to simplify the calculation the gluon fields have been rescaled as $gA \to A$.

An important point here is the different transformation properties of the quantum and background gluon fields under local SU(3) symmetry. The quantum field, after applying the BF gauge condition, transforms as $\mathcal{A}^a_\mu \to \mathcal{A}^a_\mu + f^{abc}\mathcal{A}^b_\mu \alpha^c$. Under the same symmetry, the background field transforms as you would expect an unrestricted gluon field: $A^a_\mu \to A^a_\mu + D_\mu \alpha^a$, and therefore the background field maintains local gauge invariance.

The gluon propagator in the background field method will necessarily depend on the external gluon fields. Taking the terms in the Lagrangian quadratic in $\mathcal{A}^a_\mu$, the external field propagator can be defined as the time-ordered product of quantum gluon fields:

$$\langle 0|\, \mathcal{T}\mathcal{A}^a_\mu(z)\mathcal{A}^b_\nu(0)\,|0\rangle = \overbrace{\mathcal{A}^a_\mu(z)\mathcal{A}^b_\nu}(0) = g^2\,\langle z|\left(\frac{-i}{P^2 g_{\mu\nu} + 2iG_{\mu\nu} + i\epsilon}\right)^{ab}|0\rangle \ , \tag{70}$$

where the first equality is due to Wick's theorem. The coordinate states in the term after the second equal sign are defined for some operator B as:

$$\langle x|\, B\,|y\rangle \equiv \int \frac{\mathrm{d}^d p}{(2\pi)^4} B(p) e^{-ip(x-y)} \ . \tag{71}$$

It will also be important to see the effect of the background field method on the gauge

link, which is the straight line gauge link in this calculation:

$$[x,y] = \mathcal{P}\exp\left[i\int_0^1 \mathrm{d}u(x-y)^\rho A_\rho(ux+\bar{u}y)\right] \ , \tag{72}$$

where $\bar{u} = 1-u$. The gauge field A_ρ without an explicit SU(3) index has the meaning of a gauge field contracted with an adjoint matrix: $A_\rho = T^a A^a_\rho$. Written in terms of external and quantum fields, the gauge link takes the form:

$$\begin{aligned}[x,y] = [x,y]_c &+ i\int_0^1 \mathrm{d}u(x-y)^\rho [x,ux+\bar{u}y]_c \mathcal{A}_\rho(ux+\bar{u}y)[ux+\bar{u}y,y]_c \\ &+ i^2\int_0^1 \mathrm{d}u\int_0^u \mathrm{d}v(x-y)^\rho(x-y)^\sigma [x,ux+\bar{u}y]_c \mathcal{A}_\rho(ux+\bar{u}y)[ux+\bar{u}y,vx+\bar{v}y]_c \\ &\times \mathcal{A}_\sigma(vx+\bar{v}y)[vx+\bar{v}y,y]_c + \mathcal{O}\left(g^3\right) \ ,\end{aligned} \tag{73}$$

where the subscript c is used here to denote 'classical' to differentiate between the external field gauge link, and the full gauge link. Terms of higher order than those listed in Eq. (73) will not be necessary for the calculation discussed in this text.

4.2 Fock-Schwinger gauge and Schwinger parametrization

The propagator in the form of Eq. (70) is not immediately useful, and so the Schwinger parametrization is applied:

$$\langle z|\left(\frac{-i}{P^2 g_{\mu\nu} + 2iG_{\mu\nu} + i\epsilon}\right)^{ab}|0\rangle = -\int_0^\infty \mathrm{d}s\,\langle z|\,e^{is\left(P^2 g_{\mu\nu}+2iG_{\mu\nu}+i\epsilon\right)}\,|0\rangle^{ab} \ , \tag{74}$$

where the term under the s integral is called the heat kernel, and its expansion in the new variable s is taken. After integrating back over s term by term, the resulting expansion is

well-behaved for sufficiently small values of z^2, since:

$$\int_0^\infty \mathrm{d}s s^n \left\langle z\right| e^{isp^2} \left|0\right\rangle = \frac{(-i)^n \Gamma\left(d/2-n-1\right)}{4^{n+1}\pi^2 \left(-z^2\right)^{d/2-n-1}} \ . \tag{75}$$

In other words, integrating over s and then p term by term in the expansion produces a lightcone expansion in external gluon fields.

The last piece of calculational machinery needed in order to write the gluon propagator in the desired form is the Fock-Schwinger (FS) gauge:

$$(z-z_0)^\mu A_\mu(z) = 0 \ , \tag{76}$$

where z_0 is some constant reference point that is taken to equal zero here. The FS gauge, applied to the background field, simplifies some aspects of the calculation and leads to the important (and convenient) relation between the gluon field and field strength tensor:

$$A_\nu(z) = \int_0^1 \mathrm{d}w \, w z^\mu G_{\mu\nu}(wz) \ . \tag{77}$$

Finally, the gluon propagator in external gluon fields (with adjoint indices suppressed) can be written:

$$\begin{aligned}
&\left\langle z\right| \frac{1}{P^2 g_{\alpha\beta} + 2iG_{\alpha\beta}} \left|0\right\rangle \\
&= -ig_{\alpha\beta} \frac{\Gamma(d/2-1)}{4\pi^2\left(-z^2\right)^{d/2-1}} + \frac{\Gamma(d/2-2)}{16\pi^2\left(-z^2\right)^{d/2-2}} \int_0^1 \mathrm{d}u \Big\{ 2G_{\alpha\beta}(uz) - \bar{u}uz^\nu D^\mu G_{\mu\nu}(uz) g_{\alpha\beta} \\
&\quad - 2ig_{\alpha\beta} \int_0^u \mathrm{d}v \bar{u} v z^\lambda G_{\lambda\xi}(uz) z^\rho G_\rho{}^\xi(vz) \Big\} \\
&\quad - \frac{i\Gamma(d/2-3)}{16\pi^2\left(-z^2\right)^{d/2-3}} \int_0^1 \mathrm{d}u \int_0^u \mathrm{d}v \left[G_{\alpha\xi}(uz) G_\beta{}^\xi(vz) - \tfrac{1}{2} i\bar{u} D^2 G_{\alpha\beta}(uz) \right] + \mathcal{O}\left(\text{“twist 3”}\right) \ .
\end{aligned} \tag{78}$$

It is important to note here that the above result is not a twist expansion, but that the

operators on the RHS are all those that would contribute at twist-2 for light-like separations and the appropriate choice of Lorentz indices. Furthermore, the LHS of Eq. (78) takes values of z not on the lightcone, and therefore a notion of twist cannot be defined in general for this object, and also for the gluon bilocal operator at general coordinate separation.

CHAPTER 5
GLUON BILOCAL OPERATOR

5.1 Uncontracted calculation

The calculation of corrections to the uncontracted gluon bilocal operator at one loop proceeds from the various contractions of the quantum gluon fields in:

$$\begin{aligned}
&G^a_{\mu\alpha}(z)G^a_{\nu\beta}(0) \\
&\to G^a_{\mu\alpha}(z)G^a_{\nu\beta}(0) + \left(D_\mu\mathcal{A}^a_\alpha - D_\alpha\mathcal{A}^a_\mu\right)(z)\left(D_\nu\mathcal{A}^a_\beta - D_\beta\mathcal{A}^a_\nu\right)(0) \\
&\quad + G^a_{\mu\alpha}(z)\left(D_\nu\mathcal{A}^a_\beta - D_\beta\mathcal{A}^a_\nu\right)(0) + \left(D_\mu\mathcal{A}^a_\alpha - D_\alpha\mathcal{A}^a_\mu\right)(z)G^a_{\nu\beta}(0) \\
&\quad + G^a_{\mu\alpha}(z)f^{abc}\mathcal{A}^b_\nu(0)\mathcal{A}^c_\beta(0) + f^{abc}\mathcal{A}^b_\mu(z)\mathcal{A}^c_\alpha(z)G^a_{\nu\beta}(0)\ , \qquad (79)
\end{aligned}$$

where the operator on the LHS is at renormalization point μ_2^2, and the RHS is at μ_1^2 after integration over the quantum fields, and the presence of the gauge link is implied throughout. The entirety of the RHS of Eq. (79) comes from the process of splitting the gluon field into background and quantum fields outlined in the previous chapter, and omitting terms that contribute only at higher loop level. The one contribution not entirely represented by Eq. (79) is the gluon self energy, which requires the insertion of a next order vertex, and consideration of contributions from ghost fields.

Using the methods listed in Chapter 2, the computation of the gluon bilocal operator does not rely on, or at least is not simplified by, consideration of diagrammatic representations. Nevertheless, it will be instructive to discuss the correspondence that each part of Eq. (79) has with a subset of the one-loop Feynman diagrams one would usually consider. The first term on the RHS represents the tree level contribution, in addition to the contribution from the gauge link self energy. The second term is the handbag contribution, and the two terms on the second line are the vertex contributions. The remaining two terms on the third line are one part of the self-energy diagrams.

The result for inclusion of the dual field operator, $\widetilde{G}$, is easily obtained by contraction

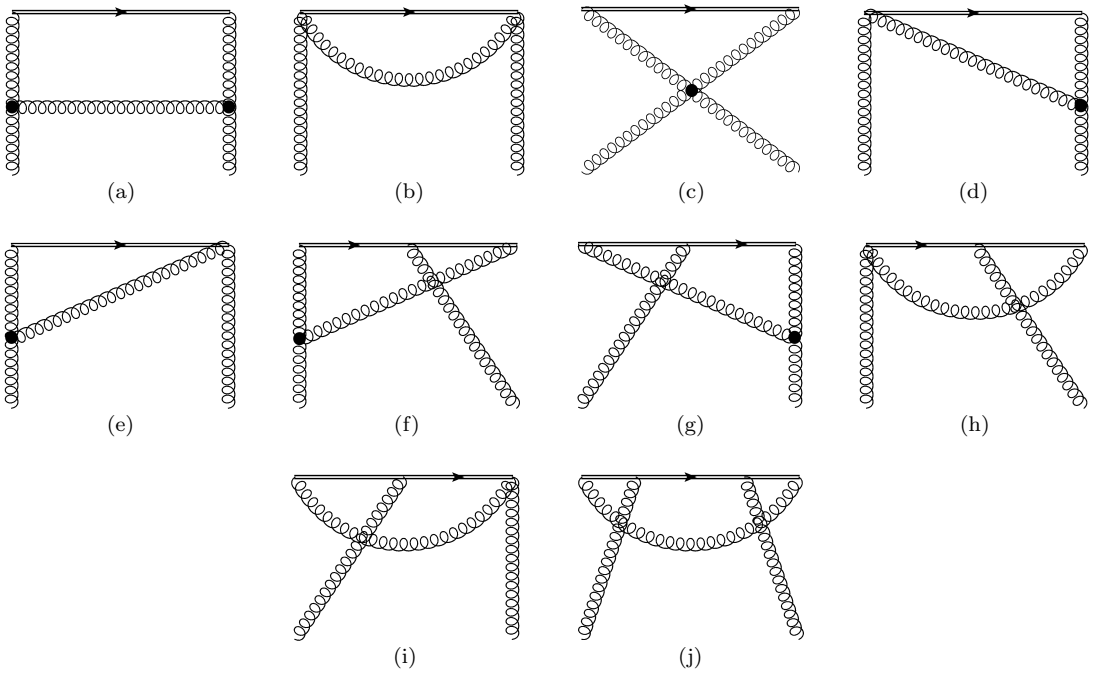

FIG. 4: Handbag diagrams. The double line represents the straight-line gauge link, here and throughout this text.

of the following results with the Levi-Civita tensor: $\frac{1}{2}\epsilon^{\rho\sigma\nu\beta}$. Since this is a straightforward operation, the explicit results of this contraction will be omitted from this text.

A major strength of performing the computation at the operator level with general Lorentz indices is its applicability to any possible matrix element. While this text will only cover the forward case in Chapter 6, it is important to note that the results listed in this chapter may be used in the consideration of nonforward objects such as generalized parton distributions (GPDs) and distribution amplitudes (DAs).

5.1.1 Handbag term

The handbag part of the calculation is given by

$$g^{-2}\left(D_\mu \mathcal{A}^a_\alpha - D_\alpha \mathcal{A}^a_\mu\right)(z)\left(D_\nu \mathcal{A}^a_\beta - D_\beta \mathcal{A}^a_\nu\right)(0)$$

$$= \langle z| \left(P_\mu \delta^\eta_\alpha - P_\alpha \delta^\eta_\mu\right) \frac{-i}{P^2 g_{\eta\xi} + 2iG_{\eta\xi}} \left(P_\nu \delta^\xi_\beta - P_\beta \delta^\xi_\nu\right) |0\rangle^{aa} \ , \tag{80}$$

and involves external gluons generated by the propagator, the end points, and the gauge link. The various terms that arise in the calculation of Eq. (80) and the source of external gluons correspond to the ten diagrams listed in Fig. 4, which are characterized by the propagator connecting the two endpoints.

The full result of the handbag calculation, written in compact notation, is:

$$\begin{aligned}
O^{\rm H}_{\mu\lambda;\nu\eta}(z) \to & \left(g_\nu{}^\sigma g_\lambda{}^\alpha g_\eta{}^\beta g_\mu{}^\rho - g_\nu{}^\sigma g_\mu{}^\alpha g_\eta{}^\beta g_\lambda{}^\rho - g_\eta{}^\sigma g_\lambda{}^\alpha g_\nu{}^\beta g_\mu{}^\rho + g_\eta{}^\sigma g_\mu{}^\alpha g_\nu{}^\beta g_\lambda{}^\rho\right) \\
& \times \left(\frac{g^2 C_A \Gamma(d/2)}{2\pi^2 \left(-z^2\right)^{d/2}} \int_0^1 {\rm d}u \int_0^u {\rm d}v g_{\alpha\beta} z_\sigma z_\rho \bar{u} v G^a_{z\xi}(uz) G^{a\xi}_z(vz) \right. \\
& + \frac{g^2 C_A \Gamma(d/2-1)}{4\pi^2 \left(-z^2\right)^{d/2-1}} \int_0^1 {\rm d}u \int_0^u {\rm d}v \Big\{ g_{\alpha\beta} \left(\bar{u} v G^a_{z\sigma}(uz) G^a_{z\rho}(vz) + \bar{v} u G^a_{z\rho}(uz) G^a_{z\sigma}(vz) \right) \\
& + \Big[z_\sigma v G^a_{\alpha\beta}(uz) G^a_{z\rho}(vz) + z_\sigma u G^a_{z\rho}(uz) G^a_{\alpha\beta}(vz) - z_\rho \bar{v} G^a_{\alpha\beta}(uz) G^a_{z\sigma}(vz) \\
& \quad - z_\rho \bar{u} G^a_{z\sigma}(uz) G^a_{\alpha\beta}(vz) \Big] \\
& + g_{\alpha\beta} \bar{u} v \Big[g_{\sigma\rho} G^a_{z\xi}(uz) G^{a\xi}_z(vz) \\
& \qquad + z_\sigma \left(G^a_{\rho\xi}(uz) G^{a\xi}_z(vz) + G^a_{z\xi}(uz) G^{a\xi}_\rho(vz) \right. \\
& \qquad\quad \left. + u D_\rho G^a_{z\xi}(uz) G^{a\xi}_z(vz) + v G^a_{z\xi}(uz) D_\rho G^{a\xi}_z(vz) \right) \\
& \qquad + z_\rho \left(G^a_{\sigma\xi}(uz) G^{a\xi}_z(vz) + G^a_{z\xi}(uz) G^{a\xi}_\sigma(vz) \right. \\
& \qquad\quad \left. - \bar{u} D_\sigma G^a_{z\xi}(uz) G^{a\xi}_z(vz) - \bar{v} G^a_{z\xi}(uz) D_\sigma G^{a\xi}_z(vz) \right) \Big] \\
& \left. + z_\sigma z_\rho G^a_{\alpha\xi}(uz) G^{a\xi}_\beta(vz) \right\} \\
& + \frac{g^2 C_A \Gamma(d/2-2)}{8\pi^2 \left(-z^2\right)^{d/2-2}} \int_0^1 {\rm d}u \int_0^u {\rm d}v \Big\{ - \bar{v} G^a_{\alpha\beta}(uz) G^a_{\rho\sigma}(vz) - \bar{u} G^a_{\rho\sigma}(uz) G^a_{\alpha\beta}(vz) \\
& - \bar{v} v G^a_{\alpha\beta}(uz) D_\rho G^a_{z\sigma}(vz) - \bar{u} u D_\rho G^a_{z\sigma}(uz) G^a_{\alpha\beta}(vz) - \bar{v} u D_\rho G^a_{\alpha\beta}(uz) G^a_{z\sigma}(vz) \\
& - \bar{u} v G^a_{z\sigma}(uz) D_\rho G^a_{\alpha\beta}(vz) - \bar{u} v D_\sigma G^a_{\alpha\beta}(uz) G^a_{z\rho}(vz) - \bar{v} u G^a_{z\rho}(uz) D_\sigma G^a_{\alpha\beta}(vz) \\
& - g_{\alpha\beta} \bar{u} v \Big[- G^a_{\sigma\xi}(uz) G^{a\xi}_\rho(vz) - G^a_{\rho\xi}(uz) G^{a\xi}_\sigma(vz) - u D_\rho G^a_{\sigma\xi}(uz) G^{a\xi}_z(vz)
\end{aligned}$$

$$
\begin{aligned}
&- v G^{a}_{\sigma\xi}(uz) D_\rho G^{a\xi}_{z}(vz) - u D_\rho G^{a}_{z\xi}(uz) G^{a\xi}_{\sigma}(vz) - v G^{a}_{z\xi}(uz) D_\rho G^{a\xi}_{\sigma}(vz) \\
&+ \bar{u} D_\sigma G^{a}_{\rho\xi}(uz) G^{a\xi}_{z}(vz) + \bar{u} D_\sigma G^{a}_{z\xi}(uz) G^{a\xi}_{\rho}(vz) + \bar{v} G^{a}_{\rho\xi}(uz) D_\sigma G^{a\xi}_{z}(vz) \\
&+ \bar{v} G^{a}_{z\xi}(uz) D_\sigma G^{a\xi}_{\rho}(vz) + u\bar{u} D_\rho D_\sigma G^{a}_{z\xi}(uz) G^{a\xi}_{z}(vz) \\
&+ v\bar{u} D_\sigma G^{a}_{z\xi}(uz) D_\rho G^{a\xi}_{z}(vz) + u\bar{v} D_\rho G^{a}_{z\xi}(uz) D_\sigma G^{a\xi}_{z}(vz) \\
&+ v\bar{v} G^{a}_{z\xi}(uz) D_\rho D_\sigma G^{a\xi}_{z}(vz) \Big] \\
&+ g_{\sigma\rho} G^{a}_{\alpha\xi}(uz) G^{a\xi}_{\beta}(vz) + u z_\sigma D_\rho G^{a}_{\alpha\xi}(uz) G^{a\xi}_{\beta}(vz) + v z_\sigma G^{a}_{\alpha\xi}(uz) D_\rho G^{a\xi}_{\beta}(vz) \\
&- \bar{u} z_\rho D_\sigma G^{a}_{\alpha\xi}(uz) G^{a\xi}_{\beta}(vz) - \bar{v} z_\rho G^{a}_{\alpha\xi}(uz) D_\sigma G^{a\xi}_{\beta}(vz) \Bigg\} \Bigg) \ . \qquad (81)
\end{aligned}
$$

The handbag term has only a logarithmic IR divergence with a straightforward expansion. Including the IR scale and $\overline{\rm MS}$ related factors, this leads to:

$$
\frac{g^2 C_A \Gamma(d/2-2)}{8\pi^2 \left(-z^2\mu^2_{\rm IR} e^{\gamma_{\rm E}}/4\pi\right)^{d/2-2}} \to \frac{g^2 C_A}{8\pi^2} \left(\frac{1}{\epsilon_{\rm IR}} - \ln\left(-z^2\mu^2 e^{2\gamma_{\rm E}}/4\right) \right) \ . \qquad (82)
$$

Also, Eq. (81) has a fairly complicated operator structure, but it simplifies considerably, at least, when considering forward matrix elements.

5.1.2 Vertex term

The vertex diagrams are split into two parts corresponding to the first and second rows in Fig. 5. The first row of diagrams, or the "left leg" diagrams, are represented by:

$$
\begin{aligned}
&g^{-2} G^{a}_{\mu\alpha}(z) \left[z,0\right]^{ab} \left(D_\nu \mathcal{A}^{b}_{\beta} - D_\beta \mathcal{A}^{b}_{\nu} \right)(0) \\
&= G^{a}_{\mu\alpha}(z) (-i f^{abc}) \int_0^1 {\rm d}u z^\eta \, \langle uz| \, \frac{-i}{P^2 g_{\eta\xi} + 2i G_{\eta\xi}} \left(P_\nu \delta^{\xi}_{\beta} - P_\beta \delta^{\xi}_{\nu} \right) |0\rangle^{bc} \ , \qquad (83)
\end{aligned}
$$

and the second row, or "right leg" diagrams are similarly represented by:

$$
g^{-2} \left(D_\mu \mathcal{A}^{a}_{\alpha} - D_\alpha \mathcal{A}^{a}_{\mu} \right)(z) \left[z,0\right]^{ab} G^{b}_{\nu\beta}(0)
$$

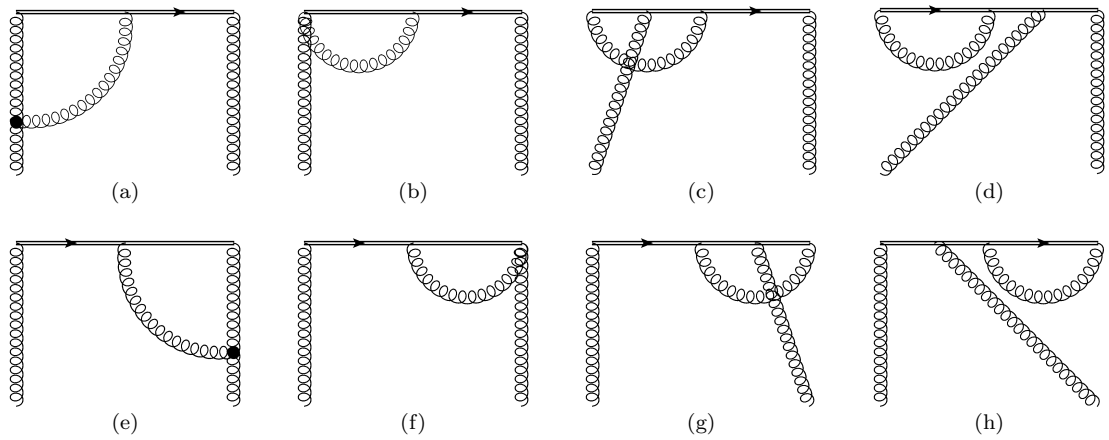

FIG. 5: Vertex diagrams.

$$= (if^{abc}) \int_0^1 \mathrm{d}u z^\xi \, \langle z| \left(P_\mu \delta^\eta_\alpha - P_\alpha \delta^\eta_\mu \right) \frac{-i}{P^2 g_{\eta\xi} + 2iG_{\eta\xi}} \, |uz\rangle^{ab} \, G^c_{\nu\beta}(0) \; . \tag{84}$$

The propagator in Eqs. (83) and (84) is constructed from a quantum field at the end point, and a quantum field coming from the gauge link, which characterizes the diagrams in Fig. 5. Both diagrams 5(a) and 5(e) involve external fields generated by the propagator. Of the remaining "left leg" diagrams, only 5(c) survives, which has an external field coming from the derivative of the gauge link. Of the remaining "right leg" diagrams, only 5(f) survives, which has an external field coming from the gluon field term of the covariant derivative. Diagrams 5(b), 5(d), and 5(h) are all zero by the FS gauge, and diagram 5(g) is zero since the derivative of the gauge link gives zero in this case.

The combined result of the left and right leg calculation is:

$$\begin{aligned} O^{\mathrm{V}}_{\mu\alpha;\nu\beta}(z) \to \frac{g^2 C_A \Gamma(d/2-1)}{4\pi^2 (-z^2)^{d/2-1}} \int_0^1 \mathrm{d}u \int_0^u \mathrm{d}v \\ \times \left\{ \delta(\bar{u}) \left(\frac{v^{3-d} - v}{d-2} \right) G^a_{\mu\alpha}(uz) \left(z_\beta G^a_{z\nu}(vz) - z_\nu G^a_{z\beta}(vz) \right) \right. \\ \left. + \delta(v) \left(\frac{\bar{u}^{3-d} - \bar{u}}{d-2} \right) \left(z_\alpha G^a_{z\mu}(uz) - z_\mu G^a_{z\alpha}(uz) \right) G^a_{\nu\beta}(vz) \right\} \end{aligned}$$

$$+\frac{g^2 C_A \Gamma(d/2-2)}{8\pi^2(-z^2)^{d/2-2}}\int_0^1 \mathrm{d}u\int_0^u \mathrm{d}v\Bigg\{\delta(\bar{u})\left[\frac{v^{3-d}-1}{d-3}\right]_{+(0)}+\delta(v)\left[\frac{\bar{u}^{3-d}-1}{d-3}\right]_{+(1)}\Bigg\}$$
$$\times G^a_{\mu\alpha}(uz)G^a_{\nu\beta}(vz)\ , \tag{85}$$

The vertex operator has both an UV and IR logarithmic divergence. The IR divergent part is on the last two lines of Eq. (85), and has the expansion:

$$\begin{aligned}
&\frac{g^2 C_A \Gamma(d/2-2)}{8\pi^2(-z^2 e^{\gamma_{\mathrm{E}}}/4\pi)^{d/2-2}}\int_0^1 \mathrm{d}u\int_0^u \mathrm{d}v\Bigg\{\delta(\bar{u})\left[\frac{v^{3-d}-1}{d-3}\right]_{+(0)}+\delta(v)\left[\frac{\bar{u}^{3-d}-1}{d-3}\right]_{+(1)}\Bigg\}\\
&\qquad\qquad\times G^a_{\mu\alpha}(uz)G^a_{\nu\beta}(vz)\\
&\to\frac{g^2 C_A}{8\pi^2}\Bigg\{\int_0^1 \mathrm{d}u\int_0^u \mathrm{d}v\left(\frac{1}{\epsilon_{\mathrm{IR}}}-\ln\left(-z^2\mu^2_{\mathrm{IR}}e^{2\gamma_{\mathrm{E}}}/4\right)\right)\left(\delta(\bar{u})\left[\frac{\bar{v}}{v}\right]_{+(0)}+\delta(v)\left[\frac{u}{\bar{u}}\right]_{+(1)}\right)\\
&\qquad+\left(\delta(\bar{u})\frac{2\bar{v}+2\ln(v)}{v}+\delta(v)\frac{2u+2\ln(\bar{u})}{\bar{u}}\right)\Bigg\}G^a_{\mu\alpha}(uz)G^a_{\nu\beta}(vz)\ .
\end{aligned}\tag{86}$$

The UV divergence comes from the local limit of the $\Gamma(d/2-1)$ term, and can be seen directly from taking the integral:

$$\int_0^1 \mathrm{d}v\frac{v^{3-d}-v}{d-2}=\frac{1}{2(4-d)}=\frac{1}{4\epsilon_{UV}}\ , \tag{87}$$

where the same can be done for the u-dependent term. The UV divergence can be isolated from the constant part, writing the constant part in terms of the plus-prescription. The UV divergent term then becomes:

$$\begin{aligned}
&\frac{g^2 C_A \Gamma(d/2-1)}{4\pi^2(-z^2)^{d/2-1}}\frac{1}{2(4-d)}\Bigg\{G^a_{\mu\alpha}(z)\left(z_\beta G^a_{z\nu}(0)-z_\nu G^a_{z\beta}(0)\right)\\
&\qquad\qquad+\left(z_\alpha G^a_{z\mu}(z)-z_\mu G^a_{z\alpha}(z)\right)G^a_{\nu\beta}(0)\Bigg\}\ ,
\end{aligned}\tag{88}$$

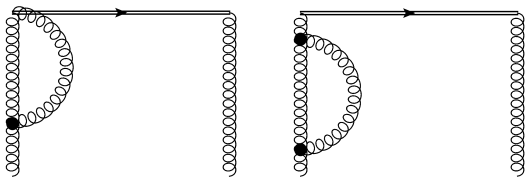

FIG. 6: Self energy type diagrams.

and has the expansion:

$$\frac{g^2 C_A}{16\pi^2(-z^2)}\left(\frac{1}{\epsilon_{\rm UV}}+\ln\left(-z^2\mu_{\rm UV}^2 e^{2\gamma_{\rm E}}/4\right)\right)\Bigg\{G^a_{\mu\alpha}(z)\left(z_\beta G^a_{z\nu}(0)-z_\nu G^a_{z\beta}(0)\right) + \left(z_\alpha G^a_{z\mu}(z)-z_\mu G^a_{z\alpha}(z)\right)G^a_{\nu\beta}(0)\Bigg\}\,. \tag{89}$$

The remainig UV constant term is:

$$\frac{g^2 C_A}{8\pi^2(-z^2)}\int_0^1 {\rm d}u\int_0^u {\rm d}v\Bigg\{\delta(\bar u)\left(\frac{1}{v}-v\right)_{+(0)} G^a_{\mu\alpha}(uz)\left(z_\beta G^a_{z\nu}(vz)-z_\nu G^a_{z\beta}(vz)\right) + \delta(v)\left(\frac{1}{\bar u}-\bar u\right)_{+(1)}\left(z_\alpha G^a_{z\mu}(uz)-z_\mu G^a_{z\alpha}(uz)\right)G^a_{\nu\beta}(vz)\Bigg\}\,. \tag{90}$$

Comparing the vertex calculation here to the 'usual way,' one might wonder about the linear divergences that would cancel after the addition of two diagrams. In the background field approach these linear divergences cancel implicitly, since the entire vertex term is treated as a single calculation. We also note here that the linear divergence in the IR part of Eq. (85), indicated by the presence of a $1/(d-3)$ term, is cancelled by the organization of the IR term into the plus-prescription, and is not the "between diagram" cancellation as suggested in [23, 24].

5.1.3 Self energy

While figs. 6(b) and 6(c) contain the actual gluon self-energy contributions, 6(a) is included due to the similarities in the calculation. The self energy type diagrams require special treatment, since they will involve terms of the form:

$$\begin{aligned}\langle z| \frac{-i}{P^2 g_{\mu\nu} + 2iG_{\mu\nu}} |z\rangle &\to -2\int \frac{\mathrm{d}^d p}{(2\pi)^4}\frac{1}{p^4} G_{\mu\nu}(z) \\ &= -\frac{i}{8\pi^2}\frac{\pi^{-\epsilon}}{\Gamma(1-\epsilon)} G_{\mu\nu}(z)\int \mathrm{d}p_\perp^2 \frac{p_\perp^{-2\epsilon}}{k_\perp^2}\ . \end{aligned} \tag{91}$$

This result is formally equal to zero in dimensional regularization and looks like the usual results one would get in the calculation of corrections to lightcone PDFs. The usual procedure here is to separate the UV part into the renormalization factor, while keeping the IR part, associated with the long distance effects, for the evolution. What remains after this procedure is a scale dependent logarithm of the form $\ln\left(\mu_{\mathrm{UV}}^2/\mu_{\mathrm{IR}}^2\right)$. In order for this result to be applicable in the pseudodistribution method the logarithm can be rewritten as: $\ln\left(-z^2\mu_{\mathrm{UV}}^2 e^{2\gamma_E}/4\right) - \ln\left(-z^2\mu_{\mathrm{IR}}^2 e^{2\gamma_E}/4\right)$, which amounts to a multiplication of the argument of $\ln\left(\mu_{\mathrm{UV}}^2/\mu_{\mathrm{IR}}^2\right)$ by 1.

Consideration of both diagrams in Fig. 6, and their right leg counterparts, leads to the following result:

$$\begin{aligned} O^S_{\mu\alpha;\nu\beta}(z) \to -\frac{g^2 C_A}{8\pi^2}&\left(\frac{1}{\epsilon_{\mathrm{IR}}} - \ln\left(-z^2\mu_{\mathrm{IR}}^2 e^{2\gamma_E}/4\right) + \frac{1}{\epsilon_{\mathrm{UV}}} + \ln\left(-z^2\mu_{\mathrm{UV}}^2 e^{2\gamma_E}/4\right)\right) \\ &\times\left[2 - \frac{\beta_0}{2C_A}\right] G_{\mu\alpha}(z) G_{\nu\beta}(0)\ , \end{aligned} \tag{92}$$

where $\beta_0 = 11C_A/3$ in gluodynamics, and substituting this value produces a factor of $1/6$ in the square brackets.

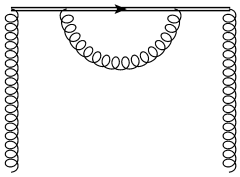

FIG. 7: Link self energy diagram.

5.1.4 Link self energy

The link self energy term is calculated from the contraction of the two quantum gluon fields in the order g^2 term of the gauge link.

$$
\begin{aligned}
& g^{-2} G^a_{\mu\alpha}(z) \left(i^2 \int_0^1 \mathrm{d}u \int_0^u \mathrm{d}v z^\rho z^\sigma \mathcal{A}_\rho(uz) \mathcal{A}_\sigma(vz) \right)^{ab} G^b_{\nu\beta}(0) \\
& = G^a_{\mu\alpha}(z) \int_0^1 \mathrm{d}u \int_0^u \mathrm{d}v z^\rho z^\sigma f^{abd} f^{bce} \langle uz | \frac{-i}{P^2 g_{\rho\sigma} + 2i G_{\rho\sigma}} | vz \rangle^{de} G^c_{\nu\beta}(0) \\
& \to -z^2 C_A \int_0^1 \mathrm{d}u \int_0^u \mathrm{d}v \langle uz | \frac{-i}{p^2} | vz \rangle G^a_{\mu\alpha}(z) G^a_{\nu\beta}(0) \ , \qquad (93)
\end{aligned}
$$

where on the last line only the leading order, and in this case relevant at twist-2, term in the propagator is kept.

It is then straightforward to obtain the result:

$$
O^{\mathrm{L}}_{\mu\alpha;\nu\beta}(z) = \frac{g^2 C_A \Gamma(d/2-1)}{4\pi^2 (-z^2)^{d/2-2}} \frac{-1}{(d-3)(d-4)} G^a_{\mu\alpha}(z) G^a_{\nu\beta}(0) \ . \qquad (94)
$$

In addition to the logarithmic UV divergence, the link self energy contribution also contains a linear UV divergence indicated by the $d-3$ in the denominator. While the presence of this linear divergence may not be relevant in dimensional regularization, it requires careful consideration in other renormalization schemes such as lattice regularization, and will come up again when discussing lattice applications in Chapter 6.

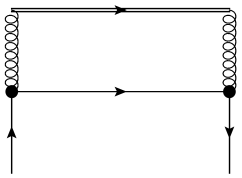

FIG. 8: Gluon quark mixing diagram.

Expansion of Eq. (94) leads to:

$$\frac{g^2 C_A}{8\pi^2}\left(\frac{1}{\epsilon_{\rm UV}}+\ln\left(-z^2\mu_{\rm UV}^2 e^{2\gamma_{\rm E}}/4\right)+2\right)G_{\mu\alpha}(z)G_{\nu\beta}(0)\ . \tag{95}$$

5.1.5 Gluon-quark mixing

The bilocal gluon operator also mixes with quark fields as one would expect. The coordinate space calculation of the gluon quark mixing requires the expansion of the gluon propagator in external quark fields, and involves the introduction of two quark gluon interaction vertices:

$$\mathcal{A}^a_\alpha(x)\mathcal{A}^a_\beta(y)\to \overbrace{\mathcal{A}^a_\alpha(x)\,i\int {\rm d}^d z_1\bar\psi(z_1)\gamma^\mu\mathcal{A}^b_\mu(z_1)t^b\phi(z_1}\,i\int {\rm d}^d z_2\bar\phi(z_2)\gamma^\nu\overbrace{\mathcal{A}^c_\nu(z_2)t^c\psi(z_2)\mathcal{A}^a_\beta(y)}\ . \tag{96}$$

Eq. (96) can then be operated on in a similar fashion to the handbag term in Eq. (80) to produce the gauge invariant result:

$$\begin{aligned}O^{GQ}_{\mu\lambda;\nu\eta}(z)\to&\left(g_\nu{}^\sigma g_\lambda{}^\alpha g_\eta{}^\beta g_\mu{}^\rho-g_\nu{}^\sigma g_\mu{}^\alpha g_\eta{}^\beta g_\lambda{}^\rho-g_\eta{}^\sigma g_\lambda{}^\alpha g_\nu{}^\beta g_\mu{}^\rho+g_\eta{}^\sigma g_\mu{}^\alpha g_\nu{}^\beta g_\lambda{}^\rho\right)\\&\times\left(\frac{ig^2C_F\Gamma(d/2)}{8\pi^2\left(-z^2\right)^{d/2}}\int_0^1{\rm d}u\int_0^u{\rm d}v z_\rho z_\sigma\Big[-\bar\psi_c(uz)\gamma_\alpha\not{z}\gamma_\beta\psi_c(vz)+\bar\psi_c(vz)\gamma_\beta\not{z}\gamma_\alpha\psi_c(uz)\Big]\right.\\&+\frac{ig^2C_F\Gamma(d/2-1)}{16\pi^2\left(-z^2\right)^{d/2-1}}\int_0^1{\rm d}u\int_0^u{\rm d}v\Big\{g_{\rho\sigma}\Big[-\bar\psi_c(uz)\gamma_\alpha\not{z}\gamma_\beta\psi_c(vz)\\&\qquad+\bar\psi_c(vz)\gamma_\beta\not{z}\gamma_\alpha\psi_c(uz)\Big]\end{aligned}$$

$$
\begin{aligned}
&+ z_\sigma \Big[- \bar\psi_c(uz) \left(u \overleftarrow{\partial}_\rho + v \overrightarrow{\partial}_\rho \right) \gamma_\alpha \not{z} \gamma_\beta \psi_c(vz) \\
&\qquad + \bar\psi_c(vz) \left(v \overleftarrow{\partial}_\rho + u \overrightarrow{\partial}_\rho \right) \gamma_\beta \not{z} \gamma_\alpha \psi_c(uz) \\
&\qquad - \bar\psi_c(uz) \gamma_\alpha \gamma_\rho \gamma_\beta \psi_c(vz) + \bar\psi_c(vz) \gamma_\beta \gamma_\rho \gamma_\alpha \psi_c(uz) \Big] \\
&- z_\rho \Big[- \bar\psi_c(uz) \left(\bar u \overleftarrow{\partial}_\sigma + \bar v \overrightarrow{\partial}_\sigma \right) \gamma_\alpha \not{z} \gamma_\beta \psi_c(vz) \\
&\qquad + \bar\psi_c(vz) \left(\bar v \overleftarrow{\partial}_\sigma + \bar u \overrightarrow{\partial}_\sigma \right) \gamma_\beta \not{z} \gamma_\alpha \psi_c(uz) \\
&\qquad + \bar\psi_c(uz) \gamma_\alpha \gamma_\sigma \gamma_\beta \psi_c(vz) - \bar\psi_c(vz) \gamma_\beta \gamma_\sigma \gamma_\alpha \psi_c(uz) \Big] \\
&- 2 z_\rho z_\sigma \Big[\bar\psi_c(uz) \left(-\bar u \overleftarrow{\partial}_\alpha \gamma_\beta + \gamma_\alpha v \overrightarrow{\partial}_\beta \right) \psi_c(vz) \\
&\qquad\qquad + \bar\psi_c(vz) \left(-v \overleftarrow{\partial}_\beta \gamma_\alpha + \gamma_\beta \bar u \overrightarrow{\partial}_\alpha \right) \psi_c(uz) \Big] \Big\} \\
&+ \frac{-ig^2 C_F \Gamma(d/2-2)}{16\pi^2 \left(-z^2\right)^{d/2-2}} \int_0^1 \mathrm{d}u \int_0^u \mathrm{d}v \Big\{ g_{\rho\sigma} \Big[\bar\psi_c(uz) \left(-\bar u \overleftarrow{\partial}_\alpha \gamma_\beta + \gamma_\alpha v \overrightarrow{\partial}_\beta \right) \psi_c(vz) \\
&\qquad\qquad + \bar\psi_c(vz) \left(-v \overleftarrow{\partial}_\beta \gamma_\alpha + \gamma_\beta \bar u \overrightarrow{\partial}_\alpha \right) \psi_c(uz) \Big] \\
&+ \frac{1}{2} \Big[- \bar\psi_c(uz) \left(\bar u u \overleftarrow{\partial}_\sigma \overleftarrow{\partial}_\rho + \bar v u \overrightarrow{\partial}_\sigma \overleftarrow{\partial}_\rho + \bar u v \overleftarrow{\partial}_\sigma \overrightarrow{\partial}_\rho + \bar v v \overrightarrow{\partial}_\sigma \overrightarrow{\partial}_\rho \right) \gamma_\alpha \not{z} \gamma_\beta \psi_c(vz) \\
&\qquad + \bar\psi_c(vz) \left(\bar v v \overleftarrow{\partial}_\sigma \overleftarrow{\partial}_\rho + \bar u v \overrightarrow{\partial}_\sigma \overleftarrow{\partial}_\rho + \bar v u \overleftarrow{\partial}_\sigma \overrightarrow{\partial}_\rho + \bar u u \overrightarrow{\partial}_\sigma \overrightarrow{\partial}_\rho \right) \gamma_\beta \not{z} \gamma_\alpha \psi_c(uz) \\
&\qquad - \bar\psi_c(uz) \left(\bar u \overleftarrow{\partial}_\sigma + \bar v \overrightarrow{\partial}_\sigma \right) \gamma_\alpha \gamma_\rho \gamma_\beta \psi_c(vz) \\
&\qquad + \bar\psi_c(vz) \left(\bar v \overleftarrow{\partial}_\sigma + \bar u \overrightarrow{\partial}_\sigma \right) \gamma_\beta \gamma_\rho \gamma_\alpha \psi_c(uz) \\
&\qquad + \bar\psi_c(uz) \left(u \overleftarrow{\partial}_\rho + v \overrightarrow{\partial}_\rho \right) \gamma_\alpha \gamma_\sigma \gamma_\beta \psi_c(vz) \\
&\qquad - \bar\psi_c(vz) \left(v \overleftarrow{\partial}_\rho + u \overrightarrow{\partial}_\rho \right) \gamma_\beta \gamma_\sigma \gamma_\alpha \psi_c(uz) \Big] \\
&+ z_\sigma \Big[\bar\psi_c(uz) \left(u \overleftarrow{\partial}_\rho + v \overrightarrow{\partial}_\rho \right) \left(-\bar u \overleftarrow{\partial}_\alpha \gamma_\beta + \gamma_\alpha v \overrightarrow{\partial}_\beta \right) \psi_c(vz) \\
&\qquad + \bar\psi_c(vz) \left(v \overleftarrow{\partial}_\rho + u \overrightarrow{\partial}_\rho \right) \left(-v \overleftarrow{\partial}_\beta \gamma_\alpha + \gamma_\beta \bar u \overrightarrow{\partial}_\alpha \right) \psi_c(uz) \Big] \\
&- z_\rho \Big[\bar\psi_c(uz) \left(\bar u \overleftarrow{\partial}_\sigma + \bar v \overrightarrow{\partial}_\sigma \right) \left(-\bar u \overleftarrow{\partial}_\alpha \gamma_\beta + \gamma_\alpha v \overrightarrow{\partial}_\beta \right) \psi_c(vz) \\
&\qquad + \bar\psi_c(vz) \left(\bar v \overleftarrow{\partial}_\sigma + \bar u \overrightarrow{\partial}_\sigma \right) \left(-v \overleftarrow{\partial}_\beta \gamma_\alpha + \gamma_\beta \bar u \overrightarrow{\partial}_\alpha \right) \psi_c(uz) \Big] \Big\} \Big) \ , \qquad (97)
\end{aligned}
$$

where $\not{z} = z^\mu \gamma_\mu$, and the derivatives act only on the fields.

The IR divergence in Eq. (97) has the same straightforward expansion seen in the case of the handbag contribution, Eq. (82).

The complicated operator structure in Eq. (97) is considerably simplified with appropriate projection on spacetime indices, and the Dirac structure may also be simplified through the use of the identity:

$$\gamma_\alpha \gamma_\sigma \gamma_\beta = \left(g_{\alpha\sigma} g_{\beta\eta} + g_{\sigma\beta} g_{\alpha\eta} - g_{\alpha\beta} g_{\sigma\eta} \right) \gamma^\eta - i \epsilon_{\alpha\sigma\beta\eta} \gamma^\eta \gamma_5 \ , \tag{98}$$

which separates out the helicity related part of the mixing term.

5.2 Multiplicative renormalizability

At spacelike separations, there are a number of multiplicatively renormalizable bilocal gluon operators in the case of two gluon field strength tensors, and in the case where one of the two is a dual tensor [29]. For $G_{\mu\alpha}(z)[z,0]G_{\nu\beta}(0)$ they are:

$$O^R_{0i;0i}(z) = Z_1^2 e^{\overline{\delta m}|z|} G_{0i}(z)[z,0]G_{0i}(0) \ , \tag{99}$$

$$O^R_{ij;ij}(z) = Z_1^2 e^{\overline{\delta m}|z|} G_{ij}(z)[z,0]G_{ij}(0) \ , \tag{100}$$

$$O^R_{3i;3i}(z) = Z_2^2 e^{\overline{\delta m}|z|} G_{3i}(z)[z,0]G_{3i}(0) \ , \tag{101}$$

$$O^R_{30;30}(z) = Z_2^2 e^{\overline{\delta m}|z|} G_{30}(z)[z,0]G_{30}(0) \ , \tag{102}$$

$$O^R_{3i;0i}(z) = Z_1 Z_2 e^{\overline{\delta m}|z|} \left(G_{3i}(z)[z,0]G_{0i}(0) + G_{0i}(z)[z,0]G_{3i}(0) \right) \ . \tag{103}$$

Similarly, the operators that include the dual tensor, $\widetilde{G}_{\mu\nu} = \frac{1}{2}\epsilon_{\mu\nu\rho\sigma} G^{\rho\sigma}$, are:

$$\tilde{O}^R_{0i;0i}(z) = Z_1 Z_2 e^{\overline{\delta m}|z|} G_{0i}(z)[z,0]\widetilde{G}_{0i}(0) \ , \tag{104}$$

$$\tilde{O}^R_{3i;3i}(z) = Z_1 Z_2 e^{\overline{\delta m}|z|} G_{3i}(z)[z,0]\widetilde{G}_{3i}(0) \ , \tag{105}$$

$$\tilde{O}^R_{ij;ij}(z) = Z_1 Z_2 e^{\overline{\delta m}|z|} G_{ij}(z)[z,0]\widetilde{G}_{ij}(0) \ , \tag{106}$$

$$\tilde{O}^R_{30;30}(z) = Z_1 Z_2 e^{\overline{\delta m}|z|} G_{30}(z)[z,0]\widetilde{G}_{30}(0) \ , \tag{107}$$

$$\tilde{O}^R_{0i;3i}(z) = Z_1^2 e^{\overline{\delta m}|z|} G_{0i}(z)[z,0]\widetilde{G}_{3i}(0) \ , \tag{108}$$

$$\tilde{O}^R_{3i;0i}(z) = Z_2^2 e^{\overline{\delta m}|z|} G_{3i}(z)[z,0]\widetilde{G}_{0i}(0) \ . \tag{109}$$

Z_1 and Z_2 are renormalization constants, and $e^{\overline{\delta m}|z|}$ is a factor related to the linear divergence in the gauge link renormalization, which can be interpreted as a mass renormalization [30]. Again, while this factor does not explicitly arise in dimensional regularization, it will come into relevance when discussing lattice applications.

5.2.1 UV vertex contribution

While the multiplicative renormalizability of the link and self energy graphs is explicit, the vertex graph is not so obvious and thus it will be useful to examine the UV part of the vertex contribution for specific cases. The general UV vertex contribution is:

$$\begin{aligned} O^{\mathrm{V,UV}}_{\mu\alpha;\nu\beta}(z) \to \frac{g^2 C_A}{16\pi^2}\left(\frac{1}{\epsilon_{\mathrm{UV}}} + \ln\left(z_3^2\mu^2_{\mathrm{UV}} e^{2\gamma_{\mathrm{E}}}/4\right)\right) \\ \times\left\{G^a_{\mu\alpha}(z)\left(z_\beta G^a_{z\nu}(0) - z_\nu G^a_{z\beta}(0)\right) + \left(z_\alpha G^a_{z\mu}(z) - z_\mu G^a_{z\alpha}(z)\right) G^a_{\nu\beta}(0)\right\} \ . \end{aligned} \tag{110}$$

The simplest cases are for $O^R_{0i;0i}$ and $O^R_{ij;ij}(z)$, since the '0' and transverse components of z are zero, and there will always be a z carrying one of these indices in both cases. Therefore, the UV vertex contribution to both of these operators is zero, and, of course, they have the same UV anomalous dimension. Next, $O^R_{3i;3i}$ and $O^R_{30;30}$ each contribute either a '0' or transverse component, but contribute a '3' component as well. Looking at Eq. (110), z_β and z_α will be zero, while z_ν and z_μ will remain. Furthermore, the terms that have z_β and z_α will also end up with G_{33}, which is also zero. Letting $\ell = 0, i$, this leads to:

$$O^{\mathrm{V,UV}}_{3\ell;3\ell}(z) \to \frac{g^2 C_A}{8\pi^2}\left(\frac{1}{\epsilon_{\mathrm{UV}}} + \ln\left(z_3^2\mu^2_{\mathrm{UV}} e^{2\gamma_{\mathrm{E}}}/4\right)\right) G^a_{3\ell}(z) G^a_{3\ell}(0) \ . \tag{111}$$

For $O^R_{3i;0i}$, only one of z_μ, z_α, z_ν, or z_β will survive for each operator. This leads to the desired result for each of the gluon operators that define $O^R_{3i;0i}$:

$$O^{\mathrm{V,UV}}_{3i;0i}(z) \to \frac{g^2 C_A}{16\pi^2}\left(\frac{1}{\epsilon_{\mathrm{UV}}} + \ln\left(z_3^2\mu^2_{\mathrm{UV}}e^{2\gamma_{\mathrm{E}}}/4\right)\right)\left(G^a_{3i}(z)G^a_{0i}(0) + G^a_{0i}(z)G^a_{3i}(0)\right) \ . \tag{112}$$

Next, looking at the cases with a dual tensor, the general UV contribution is:

$$\begin{aligned}\widetilde{O}^{\mathrm{V,UV}}_{\mu\alpha;\rho\eta}(z) \to \frac{g^2 C_A}{16\pi^2(z_3^2)}&\left(\frac{1}{\epsilon_{\mathrm{UV}}} + \ln\left(z_3^2\mu^2_{\mathrm{UV}}e^{2\gamma_{\mathrm{E}}}/4\right)\right)\\ &\times\left\{G^a_{\mu\alpha}(z)\frac{1}{2}\epsilon_{\rho\eta}{}^{\nu\beta}\left(z_\beta G^a_{z\nu}(0) - z_\nu G^a_{z\beta}(0)\right) + \left(z_\alpha G^a_{z\mu}(z) - z_\mu G^a_{z\alpha}(z)\right)\widetilde{G}^a_{\rho\eta}(0)\right\} .\end{aligned} \tag{113}$$

The simplest case here is $\widetilde{O}^R_{0i;3i}$, whose UV part is zero by the same arguments as $O^R_{0i;0i}$ and $O^R_{ij;ij}(z)$, after accounting for the presence of the Levi-Civita tensor. $\widetilde{O}^R_{3i;0i}$ then follows similarly to Eq. (111):

$$\widetilde{O}^{V,UV}_{3i;0i}(z) \to \frac{g^2 C_A}{8\pi^2}\left(\frac{1}{\epsilon_{\mathrm{UV}}} + \ln\left(z_3^2\mu^2_{\mathrm{UV}}e^{2\gamma_{\mathrm{E}}}/4\right)\right) G_{3i}(z)\widetilde{G}_{0i}(0) \ , \tag{114}$$

and the remaining operators proceed similarly to Eq. (113):

$$O^{V,UV}_{k\ell,k\ell}(z) \to \frac{g^2 C_A}{16\pi^2}\left(\frac{1}{\epsilon_{\mathrm{UV}}} + \ln\left(z_3^2\mu^2_{\mathrm{UV}}e^{2\gamma_{\mathrm{E}}}/4\right)\right) G_{k\ell}(z)\widetilde{G}_{k\ell}(0) \ , \tag{115}$$

where $(k,\ell) = (0,i),(3,i),(i,j),(3,0)$.

5.2.2 Anomalous dimensions

Combining the UV contributions from the link and self-energy type contributions to the vertex contributions outlined above, the total UV contribution can be calculated for each type of operator. The anomalous dimensions of the various operators can then be written

to order $\alpha_s = g^2/4\pi$ in the compact form:

$$\gamma\left(\alpha_s, \gamma_V\right) = -\frac{\alpha_s C_A}{4\pi}\left(\gamma_V + \frac{5}{3}\right) \ , \tag{116}$$

where γ_V is the vertex contribution and can be read off from:

$$\gamma_V = \begin{cases} 0 \ : \ O^{R,UV}_{0i;0i}, O^{R,UV}_{ij;ij}, \widetilde{O}^{R,UV}_{0i;3i} \\ 1 \ : \ O^{R,UV}_{3i;0i}, \widetilde{O}^{R,UV}_{0i;0i}, \widetilde{O}^{R,UV}_{3i;3i}, \widetilde{O}^{R,UV}_{ij;ij}, \widetilde{O}^{R,UV}_{30;30} \\ 2 \ : \ O^{R,UV}_{3i;3i}, O^{R,UV}_{30;30}, \widetilde{O}^{R,UV}_{3i;0i} \end{cases} \ . \tag{117}$$

CHAPTER 6

FORWARD MATRIX ELEMENT

Under consideration here are the unpolarized and polarized forward matrix elements:

$$M_{\mu\alpha;\nu\beta}(z,p) \equiv \langle p| \, G^a_{\mu\alpha}(z) G^a_{\nu\beta}(0) \, |p\rangle \ , \tag{118}$$

$$\widetilde{m}_{\mu\alpha;\nu\beta}(z,p) \equiv \langle p,s| \, G^a_{\mu\alpha}(z) \widetilde{G}^a_{\nu\beta}(0) \, |p,s\rangle \ , \tag{119}$$

where the external states represent some nucleon. They each admit a decomposition in terms of Lorentz invariant amplitudes that may be analyzed at arbitrary spacetime separations. By comparing the results for the spacelike case, $z = (0,0,0,z_3)$, to the lightlike case, $z^2 = 0$, a connection may be drawn between the matrix element at spacelike separations and the leading twist amplitude in the lightcone matrix element. Furthermore, the contaminating terms associated with purely higher twist effects in the lightcone limit of the spacelike matrix element are made explicit in the decomposition.

Of course, the primary motivation for calculating these matrix elements at spacelike separations is their use in the extraction of lightcone distributions from lattice calculations, i.e. the pseudodistribution method. Specifically, the results of the perturbative calculations of unpolarized and polarized gluonic matrix elements are used in the construction of the matching relations that connect the spacelike gluon correlators calculated on the lattice to lightcone gluon PDFs.

6.1 Lorentz decomposition

6.1.1 Unpolarized case

The unpolarized gluon matrix element has a decomposition in terms of six amplitudes depending on Lorentz invariants, ν and z^2:

$$M_{\mu\alpha;\nu\beta}(z,p) = \left(g_{\mu\nu}p_\alpha p_\beta - g_{\mu\beta}p_\alpha p_\nu - g_{\alpha\nu}p_\mu p_\beta + g_{\alpha\beta}p_\mu p_\nu\right) \mathcal{M}_{pp}(\nu, z^2)$$

$$
\begin{aligned}
&+ \left(g_{\mu\nu}g_{\alpha\beta} - g_{\mu\beta}g_{\alpha\nu}\right)\mathcal{M}_{gg}(\nu, z^2) \\
&+ \left(g_{\mu\nu}z_\alpha z_\beta - g_{\mu\beta}z_\alpha z_\nu - g_{\alpha\nu}z_\mu z_\beta + g_{\alpha\beta}z_\mu z_\nu\right)\mathcal{M}_{zz}(\nu, z^2) \\
&+ \left(g_{\mu\nu}z_\alpha p_\beta - g_{\mu\beta}z_\alpha p_\nu - g_{\alpha\nu}z_\mu p_\beta + g_{\alpha\beta}z_\mu p_\nu\right)\mathcal{M}_{zp}(\nu, z^2) \\
&+ \left(g_{\mu\nu}p_\alpha z_\beta - g_{\mu\beta}p_\alpha z_\nu - g_{\alpha\nu}p_\mu z_\beta + g_{\alpha\beta}p_\mu z_\nu\right)\mathcal{M}_{pz}(\nu, z^2) \\
&+ \left(p_\mu z_\alpha - p_\alpha z_\mu\right)\left(p_\nu z_\beta - p_\beta z_\nu\right)\mathcal{M}_{ppzz}(\nu, z^2)\ . \qquad (120)
\end{aligned}
$$

This result is symmetric under exchange of fields:

$$
\langle p|\, G^a_{\mu\alpha}(z)G^a_{\nu\beta}(0)\,|p\rangle = \langle p|\, G^a_{\nu\beta}(-z)G^a_{\mu\alpha}(0)\,|p\rangle\ , \qquad (121)
$$

and therefore the functions $\mathcal{M}_{pp}$, $\mathcal{M}_{gg}$, $\mathcal{M}_{zz}$, $\mathcal{M}_{ppzz}$, and $\mathcal{M}_{pz} - \mathcal{M}_{zp}$ are even functions of ν, while $\mathcal{M}_{pz} + \mathcal{M}_{zp}$ is an odd function of ν.

It will also be useful to define the unpolarized matrix element of the singlet quark bilocal operator as:

$$
\begin{aligned}
M_{S,\mu}(z,p) &= \langle p|\,\frac{i}{2}\sum_f \left(\bar\psi_f(z)\gamma_\mu\psi_f(0) - \bar\psi_f(0)\gamma_\mu\psi_f(z)\right)|p\rangle \\
&= 2p_\mu\mathcal{M}_p(\nu, z^2) + z_\mu\mathcal{M}_z(\nu, z^2)\ , \qquad (122)
\end{aligned}
$$

where the sum is over quark flavors, f.

The quark singlet forward matrix element is odd in z, so $\mathcal{M}_p$ is an odd function of ν, and $\mathcal{M}_z$ is an even function of ν.

6.1.2 Polarized case

In the polarized case one needs to also consider the spin dependence of the nucleon matrix element. The relevant object to consider is then the z-odd combination:

$$
\widetilde{M}_{\mu\alpha;\nu\beta}(z,p) \equiv \widetilde{m}_{\mu\alpha;\nu\beta}(z,p) - \widetilde{m}_{\mu\alpha;\nu\beta}(-z,p)\ , \qquad (123)
$$

which vanishes for the unpolarized case and is linear in the spin-pseudovector s. The spin-vector is normalized as $s^2 = -m^2$ for simplicity, where m is the mass of the nucleon under consideration. Additionally, since $(ps) = 0$, the 0th and 3rd components of s are $s_0 = p_3$, and $s_3 = p_0$.

It is useful to split the Lorentz decomposition into two parts, $\widetilde{M}_{\mu\alpha;\nu\beta}(z,p) \equiv \widetilde{M}^{(1)}_{\mu\alpha;\nu\beta}(z,p) + \widetilde{M}^{(2)}_{\mu\alpha;\nu\beta}(z,p)$: the first where the spin-vector takes an explicit Lorentz index:

$$\begin{aligned}
\widetilde{M}^{(1)}_{\mu\alpha;\nu\beta}(z,p) = &\left(g_{\mu\nu}s_\alpha p_\beta - g_{\mu\beta}s_\alpha p_\nu - g_{\alpha\nu}s_\mu p_\beta + g_{\alpha\beta}s_\mu p_\nu\right)\widetilde{\mathcal{M}}_{sp}(\nu,z^2) \\
&+ \left(g_{\mu\nu}p_\alpha s_\beta - g_{\mu\beta}p_\alpha s_\nu - g_{\alpha\nu}p_\mu s_\beta + g_{\alpha\beta}p_\mu s_\nu\right)\widetilde{\mathcal{M}}_{ps}(\nu,z^2) \\
&+ \left(g_{\mu\nu}s_\alpha z_\beta - g_{\mu\beta}s_\alpha z_\nu - g_{\alpha\nu}s_\mu z_\beta + g_{\alpha\beta}s_\mu z_\nu\right)\widetilde{\mathcal{M}}_{sz}(\nu,z^2) \\
&+ \left(g_{\mu\nu}z_\alpha s_\beta - g_{\mu\beta}z_\alpha s_\nu - g_{\alpha\nu}z_\mu s_\beta + g_{\alpha\beta}z_\mu s_\nu\right)\widetilde{\mathcal{M}}_{zs}(\nu,z^2) \\
&+ (p_\mu s_\alpha - p_\alpha s_\mu)(p_\nu z_\beta - p_\beta z_\nu)\widetilde{\mathcal{M}}_{pspz}(\nu,z^2) \\
&+ (p_\mu z_\alpha - p_\alpha z_\mu)(p_\nu s_\beta - p_\beta s_\nu)\widetilde{\mathcal{M}}_{pzps}(\nu,z^2) \\
&+ (s_\mu z_\alpha - s_\alpha z_\mu)(p_\nu z_\beta - p_\beta z_\nu)\widetilde{\mathcal{M}}_{szpz}(\nu,z^2) \\
&+ (p_\mu z_\alpha - p_\alpha z_\mu)(s_\nu z_\beta - s_\beta z_\nu)\widetilde{\mathcal{M}}_{pzsz}(\nu,z^2)\ , \qquad (124)
\end{aligned}$$

and the second where it appears in the scalar product (sz):

$$\begin{aligned}
\widetilde{M}^{(2)}_{\mu\alpha;\nu\beta}(z,p) = &(sz)\left(g_{\mu\nu}p_\alpha p_\beta - g_{\mu\beta}p_\alpha p_\nu - g_{\alpha\nu}p_\mu p_\beta + g_{\alpha\beta}p_\mu p_\nu\right)\widetilde{\mathcal{M}}_{pp}(\nu,z^2) \\
&+ (sz)\left(g_{\mu\nu}z_\alpha z_\beta - g_{\mu\beta}z_\alpha z_\nu - g_{\alpha\nu}z_\mu z_\beta + g_{\alpha\beta}z_\mu z_\nu\right)\widetilde{\mathcal{M}}_{zz}(\nu,z^2) \\
&+ (sz)\left(g_{\mu\nu}z_\alpha p_\beta - g_{\mu\beta}z_\alpha p_\nu - g_{\alpha\nu}z_\mu p_\beta + g_{\alpha\beta}z_\mu p_\nu\right)\widetilde{\mathcal{M}}_{zp}(\nu,z^2) \\
&+ (sz)\left(g_{\mu\nu}p_\alpha z_\beta - g_{\mu\beta}p_\alpha z_\nu - g_{\alpha\nu}p_\mu z_\beta + g_{\alpha\beta}p_\mu z_\nu\right)\widetilde{\mathcal{M}}_{pz}(\nu,z^2) \\
&+ (sz)\left(p_\mu z_\alpha - p_\alpha z_\mu\right)\left(p_\nu z_\beta - p_\beta z_\nu\right)\widetilde{\mathcal{M}}_{ppzz}(\nu,z^2) \\
&+ (sz)\left(g_{\mu\nu}g_{\alpha\beta} - g_{\mu\beta}g_{\alpha\nu}\right)\widetilde{\mathcal{M}}_{gg}(\nu,z^2)\ . \qquad (125)
\end{aligned}$$

$\widetilde{M}_{\mu\alpha;\lambda\beta}(z,p)$ is odd in z by definition, so the invariant amplitudes $\widetilde{\mathcal{M}}_{sp}, \widetilde{\mathcal{M}}_{ps}, \widetilde{\mathcal{M}}_{pzsz}, \widetilde{\mathcal{M}}_{szpz}$,

$\widetilde{\mathcal{M}}_{zp}, \widetilde{\mathcal{M}}_{pz}$ are odd functions of ν, while the remaining ones are even functions of ν.

The Lorentz decomposition for the polarized quark singlet matrix element is:

$$\begin{aligned}\widetilde{M}_{S,\mu}(z,p) &= \langle p,s| \frac{1}{2}\sum_f \left(\bar{\psi}_f(z)\gamma_\mu\gamma_5\psi_f(0) + \bar{\psi}_f(0)\gamma_\mu\gamma_5\psi_f(z)\right)|p,s\rangle \\ &= 2(sz)p_\mu\widetilde{\mathcal{M}}_p(\nu,z^2) + 2s_\mu\widetilde{\mathcal{M}}_s(\nu,z^2) + (sz)z_\mu\widetilde{\mathcal{M}}_z(\nu,z^2)\ . \end{aligned} \tag{126}$$

The matrix element here is even in z, so $\widetilde{\mathcal{M}}_p$ is odd in ν, while $\widetilde{\mathcal{M}}_s$, and $\widetilde{\mathcal{M}}_z$ are even in ν.

6.2 Lightlike separations

At lightlike seperations the matrix element is constructed from the twist-2 gluon operators: $G^a_{+i}(z)G^a_{+i}(0)$ and $G^a_{+i}(z)\widetilde{G}^a_{+i}(0)$. In this case $z=(0,z_-,0,0)$, such that $z^2 = z_+z_- = 0$. Taking the lightcone projection on the nucleon matrix elements, the invariant amplitudes associated with the leading twist behavior can be identified:

$$M_{+i;+i}(z,p) = -2p_+^2\mathcal{M}_{pp}(\nu,0) \tag{127}$$

for the unpolarized case, and

$$\begin{aligned}\widetilde{M}_{+i;+i}(z_-,p) &= -2p_+s_+\left[\widetilde{\mathcal{M}}^{(+)}_{ps}(\nu,0) + p_+z_-\widetilde{\mathcal{M}}_{pp}(\nu,0)\right] \\ &= -2p_+^2\left[\widetilde{\mathcal{M}}^{(+)}_{ps}(\nu,0) - \nu\widetilde{\mathcal{M}}_{pp}(\nu,0)\right]\end{aligned} \tag{128}$$

for the polarized. Here, $\widetilde{\mathcal{M}}^{(+)}_{ps} \equiv \widetilde{\mathcal{M}}_{ps} + \widetilde{\mathcal{M}}_{sp}$. From this result one can infer that the functions $\mathcal{M}_{pp}$, and $\widetilde{\mathcal{M}}^{(+)}_{ps} - \nu\widetilde{\mathcal{M}}_{pp}$ contain all information about twist-2 parton distributions. Furthermore, these functions are closely related to their corresponding Ioffe-time distributions (ITDs) [19], $\mathcal{I}_g$ and $\Delta\mathcal{I}_g$, and also determine the twist-2 gluon PDFs:

$$-\mathcal{M}_{pp}(\nu,0) = \mathcal{I}_{\rm g}(\nu) = \frac{1}{2}\int_{-1}^{1} {\rm d}x e^{-ix\nu} x f_g(x)$$

$$= \int_0^1 \mathrm{d}x \cos(x\nu) x f_g(x) \ , \tag{129}$$

$$i\left[\widetilde{\mathcal{M}}^{(+)}_{ps}(\nu,0) - \nu\widetilde{\mathcal{M}}_{pp}(\nu,0)\right] = \Delta\mathcal{I}_{\mathrm{g}}(\nu) = \frac{i}{2}\int_{-1}^1 \mathrm{d}x e^{-ix\nu} x\Delta g(x)$$

$$= \int_0^1 \mathrm{d}x \sin(x\nu) x\Delta g(x) \ , \tag{130}$$

where the fact that $xf_g(x)$ is even in x, and $x\Delta g(x)$ is odd in x was used in the last line of each equation.

The twist-2 quark singlet operators are $\frac{i}{2}\sum_f \left(\bar\psi_f(z)\gamma_+\psi_f(0) - \bar\psi_f(0)\gamma_+\psi_f(z)\right)$, and $\frac{1}{2}\sum_f \left(\bar\psi_f(z)\gamma_+\gamma_5\psi_f(0) + \bar\psi_f(0)\gamma_+\gamma_5\psi_f(z)\right)$ for the unpolarized and polarized cases, respectively. The forward matrix elements are then:

$$M_{S,+}(z,p) = 2p_+\mathcal{M}_p(\nu,0) \tag{131}$$

for the unpolarized case, and

$$\widetilde{M}_{S,+}(z,p) = 2p_+\left(\widetilde{\mathcal{M}}_s(\nu,0) - \nu\widetilde{\mathcal{M}}_p(\nu,0)\right) \tag{132}$$

for the polarized.

It is actually the derivatives of these matrix elements with respect to ν that are used to define the singlet ITDs for gluon-quark mixing:

$$\frac{\mathrm{d}}{\mathrm{d}\nu}\mathcal{M}_p(\nu,0) = \mathcal{I}_S(\nu)$$

$$= \int_0^1 \cos(x\nu) x f_S(x) \ , \tag{133}$$

$$\frac{\mathrm{d}}{\mathrm{d}\nu}\left(\widetilde{\mathcal{M}}_s(\nu,0) - \nu\widetilde{\mathcal{M}}_p(\nu,0)\right) = -\Delta\mathcal{I}_S(\nu)$$

$$= -\int_0^1 \mathrm{d}x \sin(x\nu) x\Delta f_S(x) \ , \tag{134}$$

where the singlet quark distributions in each case are $f_S(x) = \sum_f [q_f(x) + \bar q_f(x)]$ and

$\Delta f_S(x) = \sum_f [\Delta q_f(x) + \Delta \bar{q}_f(x)]$. Here, the fact that $x f_S(x)$ is even in x and $x\Delta f_S(x)$ is odd in x was used.

6.3 Spacelike separations

At spacelike separations the relevant projections are those discussed in Section 5.2. Because these objects are not built from operators for which twist can be defined, it is necessary to isolate the part of the Lorentz decomposition that will produce the leading twist distributions in the limit $z_3 \to 0$, and control for the contaminating terms.

6.3.1 Unpolarized case

The relevant matrix elements for the spin-averaged case are:

$$M_{0i;i0}(z,p) = 2p_0^2 \mathcal{M}_{pp}(\nu, z_3^2) + 2\mathcal{M}_{gg}(\nu, z_3^2) \ , \tag{135}$$

$$M_{ji;ij}(z,p) = -2\mathcal{M}_{gg}(\nu, z_3^2) \ , \tag{136}$$

$$M_{3i;i3}(z,p) = 2p_3^2 \mathcal{M}_{pp}(\nu, z_3^2) + 2z_3^2 \mathcal{M}_{zz}(\nu, z_3^2) \ , \tag{137}$$

$$+ 2z_3 p_3 \mathcal{M}_{pz}^{(+)}(\nu, z_3^2) - 2\mathcal{M}_{gg}(\nu, z_3^2) \ , \tag{138}$$

$$M_{30;03}(z,p) = m^2 \mathcal{M}_{pp}(\nu, z_3^2) - z_3^2 \mathcal{M}_{zz}(\nu, z_3^2) - p_0^2 z_3^2 \mathcal{M}_{ppzz}(\nu, z_3^2)$$

$$- z_3 p_3 \mathcal{M}_{pz}^{(+)}(\nu, z_3^2) + \mathcal{M}_{gg}(\nu, z_3^2) \ , \tag{139}$$

$$M_{3i;i0}(z,p) + M_{0i;i3}(z,p) = 4p_0 p_3 \mathcal{M}_{pp}(\nu, z_3^2) + 2p_0 z_3 \mathcal{M}_{pz}^{(+)}(\nu, z_3^2) \ , \tag{140}$$

where $\mathcal{M}_{pz}^{(+)} \equiv \mathcal{M}_{pz} + \mathcal{M}_{zp}$.

In Section 5.2 it was noted that $M_{0i;i0}$ and $M_{ji;ij}$ have the same anomalous dimension, as do $M_{3i;i3}$ and $M_{30;03}$; therefore, their sums must also be multiplicatively renormalizable:

$$M_{0i;i0}(z,p) + M_{ji;ij}(z,p) = 2p_0^2 \mathcal{M}_{pp}(\nu, z_3^2) \ , \tag{141}$$

$$M_{3i;i3}(z,p) + 2M_{30;03}(z,p) = 2p_0^2 \mathcal{M}_{pp}(\nu, z_3^2) - 2p_0^2 z_3^2 \mathcal{M}_{ppzz}(\nu, z_3^2) \ . \tag{142}$$

Taking these combinations leads to a reduction in the number of amplitudes that contain contributions from purely higher twist effects. In the case of $M_{0i;i0} + M_{ji;ij}$ especially, the RHS contains only the relevant twist-2 amplitude identified in Section 6.2. Additionally, the size of the remaining contaminating term in $M_{3i;i3} + 2M_{30;03}$ may be estimated by comparing it to $M_{0i;i0} + M_{ji;ij}$.

There are two possible projections for the quark singlet matrix element. They are:

$$M_{S,0}(z,p) = 2p_0 \mathcal{M}_p(\nu, z_3^2) \ , \tag{143}$$

$$M_{S,3}(z,p) = 2p_3 \mathcal{M}_p(\nu, z_3^2) + z_3 \mathcal{M}_z(\nu, z_3^2) \ . \tag{144}$$

Both of these projections will appear in the mixing term for a given projection on the gluon matrix element. The contaminating term in Eq. (144) comes with a factor of z_3, and will ideally be minimized at short distances.

6.3.2 Polarized case

The matrix elements in the polarized case are:

$$\begin{aligned}
\widetilde{M}_{0i;0i}(p,z) &= -2p_0p_3 \left(\widetilde{\mathcal{M}}^{(+)}_{sp}(\nu, z_3^2) - \nu \widetilde{\mathcal{M}}_{pp}(\nu, z_3^2) \right) + 2p_0p_3 \frac{m^2 z_3^2}{\nu} \widetilde{\mathcal{M}}_{pp}(\nu, z_3^2) \\
&\quad + 2p_0 z_3 \widetilde{\mathcal{M}}_{gg}(\nu, z_3^2) \ , \qquad (145) \\
\widetilde{M}_{ji;ji}(p,z) &= -2p_0 z_3 \widetilde{\mathcal{M}}_{gg}(\nu, z_3^2) \ , \qquad (146) \\
\widetilde{M}_{3i;3i}(p,z) &= -2p_0p_3 \left(\widetilde{\mathcal{M}}^{(+)}_{sp}(\nu, z_3^2) - \nu \widetilde{\mathcal{M}}_{pp}(\nu, z_3^2) \right) \\
&\quad - 2p_0 z_3 \left(\widetilde{\mathcal{M}}_{gg}(\nu, z_3^2) + \widetilde{\mathcal{M}}^{(+)}_{sz}(\nu, z_3^2) - z_3^2 \widetilde{\mathcal{M}}_{zz}(\nu, z_3^2) - \nu \widetilde{\mathcal{M}}^{(+)}_{zp}(\nu, z_3^2) \right) \ , \qquad (147) \\
\widetilde{M}_{30;30}(p,z) &= p_0 z_3 \Big(m^2 \widetilde{\mathcal{M}}_{pp}(\nu, z_3^2) + \widetilde{\mathcal{M}}_{gg}(\nu, z_3^2) + \widetilde{\mathcal{M}}^{(+)}_{sz}(\nu, z_3^2) - z_3^2 \widetilde{\mathcal{M}}_{zz}(\nu, z_3^2) \\
&\qquad - \nu \widetilde{\mathcal{M}}^{(+)}_{zp}(\nu, z_3^2) + m^2 \widetilde{\mathcal{M}}^{(+)}_{pspz}(\nu, z_3^2) + p_0p_3 z_3^2 \widetilde{\mathcal{M}}^{(+)}_{szpz}(\nu, z_3^2) \\
&\qquad - p_0^3 z_3^3 \widetilde{\mathcal{M}}_{ppzz}(\nu, z_3^2) \Big) \ , \qquad (148) \\
\widetilde{M}_{0i;3i}(p,z) &= -2p_0^2 \left(\widetilde{\mathcal{M}}^{(+)}_{ps}(\nu, z_3^2) - \nu \widetilde{\mathcal{M}}_{pp}(\nu, z_3^2) \right)
\end{aligned}$$

$$+ 2m^2\widetilde{\mathcal{M}}_{sp}(\nu, z_3^2) - 2\nu\widetilde{\mathcal{M}}_{sz}(\nu, z_3^2) + 2p_0^2 z_3^2\widetilde{\mathcal{M}}_{pz}(\nu, z_3^2) \ , \tag{149}$$

$$\widetilde{M}_{3i;0i}(p,z) = -2p_0^2\left(\widetilde{\mathcal{M}}^{(+)}_{ps}(\nu, z_3^2) - \nu\widetilde{\mathcal{M}}_{pp}(\nu, z_3^2)\right)$$
$$+ 2m^2\widetilde{\mathcal{M}}_{ps}(\nu, z_3^2) - 2\nu\widetilde{\mathcal{M}}_{zs}(\nu, z_3^2) + 2p_0^2 z_3^2\widetilde{\mathcal{M}}_{zp}(\nu, z_3^2) \ , \tag{150}$$

where $\widetilde{\mathcal{M}}^{(+)}_{pspz} \equiv \widetilde{\mathcal{M}}_{pspz} + \widetilde{\mathcal{M}}_{pzps}$, $\widetilde{\mathcal{M}}^{(+)}_{szpz} \equiv \widetilde{\mathcal{M}}_{szpz} + \widetilde{\mathcal{M}}_{pzsz}$, and $\widetilde{\mathcal{M}}^{(+)}_{pz} \equiv \widetilde{\mathcal{M}}_{pz} + \widetilde{\mathcal{M}}_{zp}$.

Taking advantage of symmetry under the exchange of fields, it is straightforward to show that:

$$\begin{aligned}
\widetilde{M}_{0i;0i}(p,z) &= \epsilon_{0i3j}\left\langle p\right| G_{0i}(z)G_{3j}(0) - G_{0i}(-z)G_{3j}(0)\left|p\right\rangle \\
&= -\epsilon_{0i3j}\left\langle p\right| G_{3j}(z)G_{0i}(0) - G_{3j}(-z)G_{0i}(0)\left|p\right\rangle \\
&= \widetilde{M}_{3i;3i}(p,z) \ ,
\end{aligned} \tag{151}$$

$$\begin{aligned}
\widetilde{M}_{ji;ji}(p,z) &= \epsilon_{ji30}\left\langle p\right| G_{ji}(z)G_{30}(0) - G_{ji}(-z)G_{30}(0)\left|p\right\rangle \\
&= -\epsilon_{ji30}\left\langle p\right| G_{30}(z)G_{ji}(0) - G_{30}(-z)G_{ji}(0)\left|p\right\rangle \\
&= 2\widetilde{M}_{30;30}(p,z) \ ,
\end{aligned} \tag{152}$$

which leads to the following 'sum rules' between the invariant amplitudes:

$$2\widetilde{\mathcal{M}}_{gg}(\nu, z_3^2) = -\widetilde{\mathcal{M}}^{(+)}_{zs}(\nu, z_3^2) - m^2\widetilde{\mathcal{M}}_{pp}(\nu, z_3^2) + z_3^2\widetilde{\mathcal{M}}_{zz}(\nu, z_3^2) + \nu\widetilde{\mathcal{M}}^{(+)}_{zp}(\nu, z_3^2) \ , \tag{153}$$

$$p_0^2 z_3^2\widetilde{\mathcal{M}}_{ppzz}(\nu, z_3^2) = m^2\widetilde{\mathcal{M}}^{(+)}_{pspz}(\nu, z_3^2) + \nu\widetilde{\mathcal{M}}^{(+)}_{szpz}(\nu, z_3^2) \ . \tag{154}$$

In addition to the relations shown in Eqs. (151) and (152), $\widetilde{M}_{0i;0i}$, $\widetilde{M}_{ji;ji}$, $\widetilde{M}_{3i;3i}$, and $\widetilde{M}_{30;30}$ all share the same anomalous dimension. For this reason, the following combination is also multiplicatively renormalizable:

$$\widetilde{M}_{0i;0i}(p,z) + \widetilde{M}_{ji;ji}(p,z) = -2p_0p_3\left(\widetilde{\mathcal{M}}^{(+)}_{sp}(\nu, z_3^2) - \nu\widetilde{\mathcal{M}}_{pp}(\nu, z_3^2)\right) + 2p_0p_3\frac{m^2 z_3^2}{\nu}\widetilde{\mathcal{M}}_{pp}(\nu, z_3^2) \tag{155}$$

While this result has only the the amplitudes associated with the twist-2 distribution, they are not in the desired form and so it is necessary to account for the contaminating term in some way. Because it is proportional to z_3^2, one might expect it to become negligible at small distances.

Again, there are two possible projections in the quark singlet case, and both will appear in the mixing term for some projection of the gluon matrix element. In this case, they are:

$$\widetilde{M}_{S,0}(z,p) = 2p_3\left(\widetilde{\mathcal{M}}_s(\nu,z_3^2) - \nu\widetilde{\mathcal{M}}_p(\nu,z_3^2)\right) - 2p_3\frac{m^2z_3^2}{\nu}\widetilde{\mathcal{M}}_p(\nu,z_3^2)\ , \tag{156}$$

$$\widetilde{M}_{S,3}(z,p) = 2p_0\left(\widetilde{\mathcal{M}}_s(\nu,z_3^2) - \nu\widetilde{\mathcal{M}}_p(\nu,z_3^2)\right) - p_0z_3^2\widetilde{\mathcal{M}}_z(\nu,z_3^2)\ . \tag{157}$$

Both projections result in a contaminating term that will hopefully be minimized by a strong dependence on z_3.

6.3.3 Gluon pseudo-ITD

Analogously to the lightcone case, a pseudo-ITD can be defined in terms of the invariant amplitudes at spacelike separations:

$$-\mathcal{M}_{pp}(\nu,z_3^2) = \mathcal{M}(\nu,z_3^2)\ , \tag{158}$$

$$i\left[\widetilde{\mathcal{M}}_{ps}^{(+)}(\nu,z_3^2) - \nu\widetilde{\mathcal{M}}_{pp}(\nu,z_3^2)\right] = \widetilde{\mathcal{M}}(\nu,z_3^2)\ . \tag{159}$$

One may also define pseudo-ITDs and relate them to the quark singlet amplitudes:

$$\frac{\mathrm{d}}{\mathrm{d}\nu}\mathcal{M}_p(\nu,z_3^2) = \mathcal{M}_S(\nu,z_3^2) \tag{160}$$

$$\frac{\mathrm{d}}{\mathrm{d}\nu}\left(\widetilde{\mathcal{M}}_s(\nu,z_3^2) - \nu\widetilde{\mathcal{M}}_p(\nu,z_3^2)\right) = -\widetilde{\mathcal{M}}_S(\nu,z_3^2)\ . \tag{161}$$

6.4 One-loop results

Having all the necessary machinery, it is now possible to write down the one-loop results for the gluon, including gluon-quark mixing, in terms of the invariant amplitudes defined in the previous section. The unpolarized results are:

$$
\begin{aligned}
&\frac{M_{0i;3i}(z,p)+M_{3i;0i}(z,p)}{4p_0p_3} = -\mathcal{M}_{pp}\left(\nu,z_3^2\right) - \frac{z_3^2}{2\nu}\mathcal{M}_{pz}^{(+)}\left(\nu,z_3^2\right)\\
&\to \frac{g^2C_A}{8\pi^2}\int_0^1 \mathrm{d}u\Bigg\{ \left(\frac{4}{3}\ln\!\left(z_3^2\mu_{\mathrm{UV}}^2e^{2\gamma_E}/4\right)+2\right)\delta(\bar{u}) + \left[u-3\frac{u}{\bar{u}}-4\frac{\ln(\bar{u})}{\bar{u}}\right]_{+(1)}\\
&\qquad\qquad + 2\left(\bar{u}u+\frac{2}{3}\bar{u}^3\right)\\
&\qquad\qquad - \ln\!\left(z_3^2\mu_{\mathrm{IR}}^2e^{2\gamma_E}/4\right)\left[2\bar{u}(1+u^2)+2\left[\frac{u^2}{\bar{u}}\right]_{+(1)}+\frac{1}{2}\left(\frac{\beta_0}{C_A}-6\right)\delta(\bar{u})\right]\Bigg\}\\
&\qquad\qquad \times\left(-\mathcal{M}_{pp}\left(u\nu,z_3^2\right)-\frac{z_3^2}{2\nu}\mathcal{M}_{pz}^{(+)}\left(u\nu,z_3^2\right)\right)\\
&\quad + \frac{g^2C_F}{8\pi^2}\int_0^1 \mathrm{d}u\Big\{ -2u-\ln\!\left(z_3^2\mu_{\mathrm{IR}}^2e^{2\gamma_E}/4\right)(2\bar{u}+\delta(\bar{u}))\Big\}\mathcal{M}_p(u\nu,z_3^2)/\nu\\
&\quad + \frac{g^2C_F}{8\pi^2}\int_0^1 \mathrm{d}u\Big\{ 2\left[2\bar{u}u-u^2\right]_+ - \ln\!\left(z_3^2\mu_{\mathrm{IR}}^2e^{2\gamma_E}/4\right)\left[15u^2-4u-2\right]_+\Big\}\frac{z_3^2}{\nu^2}\mathcal{M}_z(u\nu,z_3^2)\ ,
\end{aligned}
\tag{162}
$$

$$
\begin{aligned}
&\frac{M_{0i;0i}(z,p)+M_{ji;ji}(z,p)}{2p_0^2} = -\mathcal{M}_{pp}\left(\nu,z_3^2\right)\\
&\to \frac{g^2C_A}{8\pi^2}\int_0^1 \mathrm{d}u\left\{\left(\frac{5}{6}\ln\left(z_3^2\mu_{\mathrm{UV}}^2e^{2\gamma}/4\right)+2\right)\delta\left(\bar{u}\right)\right.\\
&\qquad\qquad -\left(\frac{1}{2}\delta\left(\bar{u}\right)+\left[\frac{2}{3}\left(1-u^3\right)+\frac{4u+4\ln(\bar{u})}{\bar{u}}\right]_{+(1)}\right)\\
&\qquad\qquad \left.-\ln\left(z_3^2\mu_{\mathrm{IR}}^2e^{2\gamma}/4\right)\left[2\bar{u}(1+u^2)+2\left[\frac{u^2}{\bar{u}}\right]_{+(1)}+\frac{1}{2}\left(\frac{\beta_0}{C_A}-6\right)\delta(\bar{u})\right]\right\}\\
&\qquad\qquad \times\left(-\mathcal{M}_{pp}\left(u\nu,z_3^2\right)\right)
\end{aligned}
$$

$$
\begin{aligned}
&+\frac{g^2 C_A}{8\pi^2}\int_0^1 \mathrm{d}u\left\{-\frac{2}{3}\left(1-u^3\right)-\ln\left(z_3^2\mu_{\mathrm{IR}}^2 e^{2\gamma}/4\right)\bar{u}\left(u^2+1\right)\right\}u^2 z_3^2\mathcal{M}_{ppzz}\left(u\nu,z_3^2\right)\\
&+\frac{g^2 C_F}{8\pi^2}\int_0^1 \mathrm{d}u\left\{-\ln\left(z_3^2\mu_{\mathrm{IR}}^2 e^{2\gamma_E}/4\right)\left(2\bar{u}+\delta(\bar{u})\right)\right\}\mathcal{M}_p(u\nu,z_3^2)/\nu\\
&+\frac{g^2 C_F}{8\pi^2}\int_0^1 \mathrm{d}u\left\{\ln\left(z_3^2\mu_{\mathrm{IR}}^2 e^{2\gamma_E}/4\right)6\Big[u^2-\bar{u}u\Big]_{+(1)}\right\}\frac{z_3^2}{\nu^2}\mathcal{M}_z(u\nu,z_3^2)\ , \qquad (163)
\end{aligned}
$$

$$
\begin{aligned}
&\frac{M_{3i;3i}(z,p)+M_{30;30}(z,p)}{2p_0^2}=-\mathcal{M}_{pp}\left(\nu,z_3^2\right)+2p_0^2 z_3^2\mathcal{M}_{ppzz}\left(\nu,z_3^2\right)\\
&\to\frac{g^2 C_A}{8\pi^2}\int_0^1 \mathrm{d}u\left\{\left(\frac{11}{6}\ln\left(z_3^2\mu_{\mathrm{UV}}^2 e^{2\gamma}/4\right)+2\right)\delta\left(\bar{u}\right)\right.\\
&\qquad\qquad-\left(\frac{1}{2}\delta\left(\bar{u}\right)+\left[\frac{2}{3}\left(1-u^3\right)+\frac{2u^2+4\ln(\bar{u})}{\bar{u}}\right]_{+(1)}\right)\\
&\qquad\qquad\left.-\ln\left(z_3^2\mu_{\mathrm{IR}}^2 e^{2\gamma}/4\right)\left[2\bar{u}(1+u^2)+2\left[\frac{u^2}{\bar{u}}\right]_{+(1)}+\frac{1}{2}\left(\frac{\beta_0}{C_A}-6\right)\delta(\bar{u})\right]\right\}\\
&\qquad\qquad\times\left(-\mathcal{M}_{pp}\left(u\nu,z_3^2\right)+u^2 z_3^2\mathcal{M}_{ppzz}\left(u\nu,z_3^2\right)\right)\\
&+\frac{g^2 C_A}{8\pi^2}\int_0^1 \mathrm{d}u\left\{2\bar{u}+\ln\left(z_3^2\mu_{\mathrm{IR}}^2 e^{2\gamma}/4\right)\bar{u}\left(u^2+1\right)\right\}u^2 z_3^2\mathcal{M}_{ppzz}\left(u\nu,z_3^2\right)\\
&+\frac{g^2 C_F}{8\pi^2}\int_0^1 \mathrm{d}u\left\{-4-\ln\left(z_3^2\mu_{\mathrm{IR}}^2 e^{2\gamma_E}/4\right)\left(2\bar{u}+\delta(\bar{u})\right)\right\}\mathcal{M}_p(u\nu,z_3^2)/\nu\\
&+\frac{g^2 C_F}{8\pi^2}\int_0^1 \mathrm{d}u\left\{\ln\left(z_3^2\mu_{\mathrm{IR}}^2 e^{2\gamma_E}/4\right)\left(9u^2-12u+2\right)\right\}\frac{z_3^2}{\nu^2}\mathcal{M}_z(u\nu,z_3^2)\ . \qquad (164)
\end{aligned}
$$

All three combinations carry the expected coordinate space DGLAP evolution kernels for gluon-gluon and gluon-quark:

$$
B_{gg}(u)=2\bar{u}(1+u^2)+2\left[\frac{u^2}{\bar{u}}\right]_{+(1)}+\frac{1}{2}\left(\frac{\beta_0}{C_A}-6\right),\qquad B_{gq}=\delta(\bar{u})+2\bar{u} \qquad (165)
$$

Setting $\beta_0=11C_A/3$, the gluon-gluon kernel takes the plus prescription form:

$$
B_{gg}(u)=\left[\frac{2(1-u\bar{u})^2}{\bar{u}}\right]_{+(1)}\ , \qquad (166)
$$

necessary for momentum conservation of the gluon.

Of the three combination Eq. (163) is the only one with the desired amplitude isolated on the LHS. Furthermore, there are minimal contaminating terms on the RHS, and both come with a z_3^2 factor and should be minimized at short distances.

The one-loop contributions in the polarized case are:

$$
\begin{aligned}
\frac{\widetilde{M}_{0i;3i}(p,z)}{2p_0^2} &= -\left(\widetilde{\mathcal{M}}_{sp}^{(+)}(\nu,z_3^2) - \nu\widetilde{\mathcal{M}}_{pp}(\nu,z_3^2)\right) + \widetilde{\mathcal{M}}_{spz}(\nu,z_3^2) \\
&\to \frac{g^2C_A}{8\pi^2}\int_0^1 \mathrm{d}u\Bigg\{ \left(\frac{5}{6}\ln\left(z_3^2\mu_{\mathrm{UV}}^2 e^{2\gamma}/4\right)+2\right)\delta(\bar{u}) + 2u\bar{u} - 4\left[\frac{u+\ln(1-u)}{\bar{u}}\right]_{+(1)} \\
&\qquad - \ln\left(z_3^2\mu_{\mathrm{IR}}^2 e^{2\gamma}/4\right)\left[4\bar{u}u + 2\left[\frac{u^2}{\bar{u}}\right]_{+(1)} + \frac{1}{2}\left(\frac{\beta_0}{C_A}-6\right)\delta(\bar{u})\right]\Bigg\} \\
&\qquad \times\left(-\left(\widetilde{\mathcal{M}}_{sp}^{(+)}(u\nu,z_3^2) - u\nu\widetilde{\mathcal{M}}_{pp}(u\nu,z_3^2)\right) + \widetilde{\mathcal{M}}_{spz}(u\nu,z_3^2)\right) \\
&+ \frac{g^2C_A}{8\pi^2}\int_0^1 \mathrm{d}u\left\{2u\bar{u} + \ln\left(z_3^2\mu_{\mathrm{IR}}^2 e^{2\gamma}/4\right)\bar{u}\right\}\widetilde{\mathcal{M}}_{zps}^{(-)}(u\nu,z_3^2) \\
&+ \frac{g^2C_F}{8\pi^2}\int_0^1 \mathrm{d}u\left\{ -2\bar{u} - \ln\left(z_3^2\mu_{\mathrm{IR}}^2 e^{2\gamma_E}/4\right)\left(2\bar{u}-\delta(\bar{u})\right)\right\} \\
&\qquad \times\left(\widetilde{\mathcal{M}}_s(u\nu,z_3^2) - u\nu\widetilde{\mathcal{M}}_p(u\nu,z_3^2)\right)/\nu \\
&+ \frac{g^2C_F}{8\pi^2}\int_0^1 \mathrm{d}u 2\bar{u}\frac{m^2}{p_0^2}\widetilde{\mathcal{M}}_s(u\nu,z_3^2)/\nu \\
&+ \frac{g^2C_F}{8\pi^2}\ln\left(z_3^2\mu_{\mathrm{IR}}^2 e^{2\gamma_E}/4\right)\int_0^1 \mathrm{d}u\, 6(u^2-\bar{u}u)_+\frac{m^2z_3^2}{\nu^2}\widetilde{\mathcal{M}}_p(u\nu,z_3^2) \\
&+ \frac{g^2C_F}{8\pi^2}\ln\left(z_3^2\mu_{\mathrm{IR}}^2 e^{2\gamma_E}/4\right)\int_0^1 \mathrm{d}u\, 2(3\bar{u}u^2-u^3)_+\frac{z_3^2}{\nu}\widetilde{\mathcal{M}}_z(u\nu,z_3^2)\ , \qquad (167)
\end{aligned}
$$

$$
\begin{aligned}
\frac{\widetilde{M}_{3i;0i}(p,z)}{2p_0^2} &= -\left(\widetilde{\mathcal{M}}_{sp}^{(+)}(\nu,z_3^2) - \nu\widetilde{\mathcal{M}}_{pp}(\nu,z_3^2)\right) + \widetilde{\mathcal{M}}_{zps}(\nu,z_3^2) \\
&\to \frac{g^2C_A}{8\pi^2}\int_0^1 \mathrm{d}u\Bigg\{ \left(\frac{11}{6}\ln\left(z_3^2\mu_{\mathrm{UV}}^2 e^{2\gamma}/4\right)+2\right)\delta(\bar{u}) + 2\bar{u}u \\
&\qquad - 4\left[\frac{u+\ln(1-u)}{\bar{u}}\right]_{+(1)} + 2\left[\frac{1}{\bar{u}}-\bar{u}\right]_{+(1)}
\end{aligned}
$$

$$
\begin{aligned}
&\quad - \ln\left(z_3^2\mu_{\rm IR}^2 e^{2\gamma}/4\right)\left[4\bar{u}u + 2\left[\frac{u^2}{\bar{u}}\right]_{+(1)} + \frac{1}{2}\left(\frac{\beta_0}{C_A} - 6\right)\delta(\bar{u})\right]\Bigg\} \\
&\quad \times \left(-\left(\widetilde{\mathcal{M}}_{sp}^{(+)}(u\nu, z_3^2) - u\nu\widetilde{\mathcal{M}}_{pp}(u\nu, z_3^2)\right) + \widetilde{\mathcal{M}}_{zps}(u\nu, z_3^2)\right) \\
&+ \frac{g^2 C_A}{8\pi^2}\int_0^1 {\rm d}u\Bigg\{ - 2\bar{u} - \ln\left(z_3^2\mu_{\rm IR}^2 e^{2\gamma}/4\right)\bar{u}\Bigg\}\widetilde{\mathcal{M}}_{zps}^{(-)}(u\nu, z_3^2) \\
&+ \frac{g^2 C_F}{8\pi^2}\int_0^1 {\rm d}u\Bigg\{2\left(1+u\right) - \ln\left(z_3^2\mu_{\rm IR}^2 e^{2\gamma_E}/4\right)\left(2\bar{u} - \delta(\bar{u})\right)\Bigg\} \\
&\quad \times \left(\left(\widetilde{\mathcal{M}}_s(\nu, z_3^2) - \nu\widetilde{\mathcal{M}}_p(\nu, z_3^2)\right)/\nu - \frac{m^2}{p_0^2}\widetilde{\mathcal{M}}_s(\nu, z_3^2)/\nu\right) \ , \qquad (168)
\end{aligned}
$$

$$
\begin{aligned}
&\frac{\widetilde{M}_{0i;0i}(z,p) + \widetilde{M}_{ij;ij}(z,p)}{2p_0 p_3} = -\left(\widetilde{\mathcal{M}}_{sp}^{(+)}(\nu, z_3^2) - \nu\widetilde{\mathcal{M}}_{pp}(\nu, z_3^2)\right) + \frac{m^2 z_3^2}{\nu}\widetilde{\mathcal{M}}_{pp}(\nu, z_3^2) \\
&\to \frac{g^2 C_A}{8\pi^2}\int_0^1 {\rm d}u\Bigg\{\left(\frac{4}{3}\ln\left(z_3^2\mu_{\rm UV}^2 e^{2\gamma_E}/4\right) + 2\right)\delta(\bar{u}) \\
&\quad - 2\bar{u}u - 4\left[\frac{u + \ln(1-u)}{\bar{u}}\right]_{+(1)} + \left(\frac{1}{\bar{u}} - \bar{u}\right)_{+(1)} \\
&\quad - \ln\left(z_3^2\mu_{\rm IR}^2 e^{2\gamma_E}/4\right)\left[4\bar{u}u + 2\left[\frac{u^2}{\bar{u}}\right]_{+(1)} + \frac{1}{2}\left(\frac{\beta_0}{C_A} - 6\right)\delta(\bar{u})\right]\Bigg\} \\
&\quad \times \left(-\left(\widetilde{\mathcal{M}}_{sp}^{(+)}(u\nu, z_3^2) - u\nu\widetilde{\mathcal{M}}_{pp}(u\nu, z_3^2)\right) + u\frac{m^2 z_3^2}{\nu}\widetilde{\mathcal{M}}_{pp}(u\nu, z_3^2)\right) \\
&+ \frac{g^2 C_F}{8\pi^2}\int_0^1 {\rm d}u\Bigg\{ - 2(1-2u) - \ln\left(z_3^2\mu_{\rm IR}^2 e^{2\gamma_E}/4\right)\left(2\bar{u} - \delta(\bar{u})\right)\Bigg\} \\
&\quad \times \left(\widetilde{\mathcal{M}}_s(u\nu, z_3^2) - u\nu\widetilde{\mathcal{M}}_p(u\nu, z_3^2)\right)/\nu \\
&+ \frac{g^2 C_F}{8\pi^2}\int_0^1 {\rm d}u\Bigg\{2\left[2\bar{u}u - u^2\right]_{+(1)} + \ln\left(z_3^2\mu_{\rm IR}^2 e^{2\gamma_E}/4\right)\left[(4\bar{u}u + u^2)\right]_{+(1)}\Bigg\} \\
&\quad \times \frac{m^2 z_3^2}{\nu^2}\widetilde{\mathcal{M}}_p(u\nu, z_3^2) \ , \qquad (169)
\end{aligned}
$$

where the following simplifications were made in Eqs. (167) and (168):

$$
2p_0^2\widetilde{\mathcal{M}}_{spz}(\nu, z_3^2) = 2m^2\widetilde{\mathcal{M}}_{sp}(\nu, z_3^2) - 2\nu\widetilde{\mathcal{M}}_{sz}(\nu, z_3^2) + 2p_0^2 z_3^2\widetilde{\mathcal{M}}_{pz}(\nu, z_3^2) \ ,
$$

$$2p_0^2\widetilde{\mathcal{M}}_{zps}(\nu,z_3^2) = 2m^2\widetilde{\mathcal{M}}_{ps}(\nu,z_3^2) - 2\nu\widetilde{\mathcal{M}}_{zs}(\nu,z_3^2) + 2p_0^2z_3^2\widetilde{\mathcal{M}}_{zp}(\nu,z_3^2)\ ,$$
$$2p_0^2\widetilde{\mathcal{M}}^{(-)}_{zps}(\nu,z_3^2) = 2m^2\widetilde{\mathcal{M}}^{(-)}_{ps}(\nu,z_3^2) - 2\nu\widetilde{\mathcal{M}}^{(-)}_{zs}(\nu,z_3^2) + 2p_0^2z_3^2\widetilde{\mathcal{M}}^{(-)}_{zp}(\nu,z_3^2)\ . \tag{170}$$

Again, the expected AP kernels appear for gluon-gluon and gluon-quark:

$$\widetilde{B}_{gg}(u) = 4\bar{u}u + 2\left[\frac{u^2}{\bar{u}}\right]_{+(1)} + \frac{1}{2}\left(\frac{\beta_0}{C_A} - 6\right)\delta(\bar{u}), \qquad \widetilde{B}_{gq} = \delta(\bar{u}) - 2\bar{u} \tag{171}$$

The most promising combination is Eq. (169), where all the contaminating terms come with a factor of z_3^2. In principle, by measuring this matrix element at constant ν for small values of z_3^2, the behavior of the "twist-2" part may be isolated. The presence of a momentum factor multiplying the amplitude, however, will lead to complications when constructing the matching conditions in Section 6.5.2. The other two combinations, Eqs. (167) and (168) are attractive then, because they come with a factor of p_0^2. However, the contaminating terms in both cases don't all carry an explicit factor of z_3^2, and it remains to be seen if $\widetilde{\mathcal{M}}_{spz}$ and $\widetilde{\mathcal{M}}_{zps}$ are minimized at small distances.

6.5 Evolution and matching

6.5.1 Gluon PDF

For the case of the gluon PDF, Eq. (163) is used to construct the matching relation. The construction of the pseudo-rITD is straightforward in this case since it comes with a factor of p_0^2, and is therefore finite in the rest frame. The ratio is:

$$\mathfrak{M}(\nu,z_3^2) = \frac{M_{0i;0i}(z,p) + M_{ji;ji}(z,p)}{M_{0i;0i}(z,p_3=0) + M_{ji;ji}(z,p_3=0)} = \frac{\mathcal{M}_{pp}\left(\nu,z_3^2\right)}{\mathcal{M}_{pp}\left(0,z_3^2\right)}\ . \tag{172}$$

From here, it is straightforward to perform an expansion around α_s in order to obtain the ratio at leading order.

As discussed, the UV associated terms cancel entirely in the ratio method, and conse-

quently all dependence on z_3^2 is in the evolution logarithm, leading to an evolution equation at short distances:

$$\begin{aligned}\frac{\mathrm{d}\mathfrak{M}(\nu,z_3^2)}{\mathrm{d}\ln z_3^2} = &-\frac{\alpha_s C_A}{2\pi}\int_0^1 \mathrm{d}u B_{gg}(u)\mathfrak{M}\left(u\nu,z_3^2\right)\\ &-\frac{\alpha_s C_F}{2\pi}\int_0^1 \mathrm{d}u\mathcal{B}_{gq}(u)\left(\mathfrak{M}_S(u\nu,z_3^2)-\mathfrak{M}\left(\nu,z_3^2\right)\mathfrak{M}_S(0,z_3^2)\right)\\ &+\mathcal{O}\left(z_3^2m^2,z_3^2\Lambda_{\mathrm{QCD}}\right)\ ,\end{aligned} \tag{173}$$

where the kernel $\mathcal{B}_{gq}(u)$ results from transforming the gluon-quark mixing amplitude to its rITD counterpart and is obtained directly from:

$$\mathcal{B}_{gq}(u)=\int_u^1 \mathrm{d}v B_{gq}(v)=1+\bar{u}^2 \tag{174}$$

Also, the contaminating terms on the RHS of Eq. (163) have been absorbed into the $\mathcal{O}\left(z_3^2m^2,z_3^2\Lambda_{\mathrm{QCD}}\right)$ term.

A peculiar aspect of the pseudo-rITD evolution equation is the presence of the product $\mathfrak{M}\left(\nu,z_3^2\right)\mathfrak{M}_S(0,z_3^2)$ in the mixing term, which is purely a result of the ratio method. Here, the singlet pseudo-rITD is defined as:

$$\mathfrak{M}_S(\nu,z_3^2)=\frac{\mathcal{M}_S(\nu,z_3^2)}{\mathcal{M}_{pp}(0,z_3^2)} \tag{175}$$

The matching relation for the gluon PDF can be written in terms of ITDs as:

$$\begin{aligned}\mathfrak{M}(\nu,z_3^2)=\frac{\mathcal{I}_g(\nu,\mu^2)}{\mathcal{I}_g(0,\mu^2)}&-\frac{\alpha_s C_A}{2\pi}\int_0^1\mathrm{d}u\Bigg\{\left[\frac{2}{3}\left(1-u^3\right)+\frac{4u+4\ln(\bar{u})}{\bar{u}}\right]_{+(1)}\\ &+\ln\left(z_3^2\mu^2e^{2\gamma}/4\right)B_{gg}(u)\Bigg\}\frac{\mathcal{I}_g(u\nu,\mu^2)}{\mathcal{I}_g(0,\mu^2)}\\ &-\frac{\alpha_s C_F}{2\pi}\ln\left(z_3^2\mu^2e^{2\gamma_E}/4\right)\int_0^1\mathrm{d}u\mathcal{B}_{gq}(u)\left(\frac{\mathcal{I}_S(u\nu,\mu^2)}{\mathcal{I}_g(0,\mu^2)}-\frac{\mathcal{I}_g(\nu,\mu^2)}{\mathcal{I}_g(0,\mu^2)}\frac{\mathcal{I}_S(0,\mu^2)}{\mathcal{I}_g(0,\mu^2)}\right)\\ &+\mathcal{O}\left(z_3^2m^2,z_3^2\Lambda_{\mathrm{QCD}}\right)\ .\end{aligned} \tag{176}$$

However, it is straightforward to rewrite the RHS of Eq. (176) in terms of the gluon PDF and quark singlet PDF, since the lightcone ITDs are directly related to the lightcone PDFs (Eqs. (129) and (133)). Making these substitutions, the matching relation becomes:

$$\mathfrak{M}(\nu, z_3^2) = \int_0^1 \mathrm{d}x \frac{x f_g(x,\mu^2)}{\langle x \rangle_{\mu^2}} \left(R_{gg}(x\nu, z_3^2\mu^2) + R_r(x\nu, z_3^2\mu^2) \frac{\langle x_S \rangle_{\mu^2}}{\langle x \rangle_{\mu^2}} \right) + \int_0^1 \mathrm{d}x \frac{x f_S(x,\mu^2)}{\langle x \rangle_{\mu^2}} R_{gq}(x\nu, z_3^2\mu^2) + \mathcal{O}\left(z_3^2 m^2, z_3^2 \Lambda_{\mathrm{QCD}}\right) \ , \tag{177}$$

where it was used that $\mathcal{I}_g(0,\mu^2) = \langle x \rangle_{\mu^2}$ and $\mathcal{I}_S(0,\mu^2) = \langle x_S \rangle_{\mu^2}$, the hadron momentum fractions carried by the gluons and quarks, respectively. The three functions, R_{gg}, R_{gq}, and R_r can be directly calculated from the cosine transformation of the u dependent parts of Eq. (176). They are:

$$R_{gg}(x\nu, z_3^2\mu^2) = \int_0^1 \mathrm{d}u \cos(ux\nu) \left(\delta(\bar{u}) - \frac{\alpha_s C_A}{2\pi} \left\{ \left(\left[\frac{2}{3}\left(1-u^3\right) + \frac{4u + 4\ln(\bar{u})}{\bar{u}} \right]_{+(1)} \right) + \ln\left(z_3^2\mu^2 e^{2\gamma}/4\right) B_{gg}(u) \right\} \right) \ , \tag{178}$$

$$R_{gq}(x\nu, z_3^2\mu^2) = \int_0^1 \mathrm{d}u \cos(ux\nu) \left(-\frac{\alpha_s C_F}{2\pi} \ln\left(z_3^2\mu^2 e^{2\gamma_E}/4\right) \mathcal{B}_{gq}(u) \right) \ , \tag{179}$$

$$R_r(x\nu, z_3^2\mu^2) = \frac{4}{3}\cos(x\nu) \frac{\alpha_s C_F}{2\pi} \ln\left(z_3^2\mu^2 e^{2\gamma_E}/4\right) \ . \tag{180}$$

The last of these, R_r comes from the extra ratio related factor in the mixing term, hence the 4/3 factor that comes from the integral of the mixing kernel. Since they are calculated from the cosine transformation of perturbatively calculated matching coefficients, the R kernels themselves are explicitly perturbatively calculable expressions.

The gluonic part of the unpolarized matching relation has already been used in the lattice extraction of the gluon PDF by the HadStruc collaboration at Jefferson Lab, Fig. 9 [35]. The data given in Fig. 9 is limited by the range in ν for which the pseudo-rITD has been calculated on the lattice, $\nu \in [0, 7.07]$. This especially leads to uncertainty in the small-x

region. Lattice calculations at greater values of ν are necessary to improve the gluon PDF extraction [36]. The lattice group at Michigan State University has also performed a lattice extraction of the gluon PDF using the matching relations given in this text, [37, 38]. It should be stressed that the results of both groups are obtained from first principles calculations in QCD.

6.5.2 Polarized gluon PDF

The pseudo-rITD is not so easily constructed in the polarized case because of the factor of p_3 that multiplies the amplitude, leading to a division by zero. One way to approach this is to use a different matrix element in the denominator, and this is chosen to be the spin average combination $M_{0i;0i}(z, p_3 = 0) + M_{ji;ji}(z, p_3 = 0)$, giving the ratio:

$$\frac{\widetilde{M}_{0i;0i}(z,p) + \widetilde{M}_{ji;ji}(z,p)}{M_{0i;0i}(z,p_3=0) + M_{ji;ji}(z,p_3=0)} \ . \tag{181}$$

While this ratio has the desired effect of canceling the linear divergence, in addition to the UV logarithms coming from the self energy and gauge link, there is a mismatch between UV factors associated with the vertex diagrams. Using the terminology from Section 5.2.2: the numerator has $\gamma_V = 1$, while the denominator has $\gamma_V = 0$. In order to compensate for this mismatch, a multiplicative factor associated with all orders exponentiation of the UV logarithms in the vertex diagram is introduced. On the lattice, this factor is:

$$Z_{\mathrm{L}}(z_3/a_L) = \left(1 + \pi^2 z_3^2/a_L^2\right)^{\alpha_s C_A/4\pi} \ , \tag{182}$$

Accounting for this factor leads to the modified ratio:

$$\widetilde{\mathfrak{M}}(\nu, z_3^2) \equiv \frac{\left(\widetilde{M}_{0i;0i}(z,p) + \widetilde{M}_{ji;ji}(z,p)\right)/(p_0 p_3)}{iZ_{\mathrm{L}}(z_3/a_L)\left(M_{0i;0i}(z,p_3=0) + M_{ji;ji}(z,p_3=0)\right)/m^2} \ , \tag{183}$$

which gives the necessary properties for the evolution equation:

$$\begin{aligned}\frac{\mathrm{d}\widetilde{\mathfrak{M}}(\nu,z_3^2)}{\mathrm{d}\ln z_3^2} &= -\frac{\alpha_s C_A}{2\pi}\int_0^1 \mathrm{d}u\widetilde{\mathcal{B}}_{gg}(u)\widetilde{\mathfrak{M}}(u\nu,z_3^2)\\ &\quad -\frac{\alpha_s C_A}{2\pi}\int_0^1 \mathrm{d}u\widetilde{\mathcal{B}}_{gq}(u)\left(\widetilde{\mathfrak{M}}_S(u\nu,z_3^2)-2\,\mathfrak{M}_S(0,z_3^2)\widetilde{\mathfrak{M}}(\nu,z_3^2)\right)\\ &\quad +\mathcal{O}\left(z_3^2m^2,z_3^2\Lambda_{\mathrm{QCD}}\right)\ . \end{aligned} \tag{184}$$

The kernel, $\widetilde{\mathcal{B}}_{gg}$, technically has the same value as the AP kernel, but here the dependence on β_0 has explicitly canceled in the ratio. Also, the gluon-quark kernel is, again, the result of transforming the gluon-quark mixing amplitude to its associated rITD.

$$\widetilde{\mathcal{B}}_{gg}(u)=2\left[2\bar{u}u+\frac{u^2}{\bar{u}}\right]_{+(1)}-\frac{1}{2}\delta(\bar{u}),\qquad \widetilde{\mathcal{B}}_{gq}(u)=\int_u^1 \mathrm{d}v\widetilde{B}_{gq}(v)=1-\bar{u}^2\ . \tag{185}$$

$\mathfrak{M}_S$ is defined by Eq. (175), and the singlet quark polarized pseudo-rITD is:

$$\widetilde{\mathfrak{M}}_S(\nu,z_3^2)=\frac{\widetilde{\mathcal{M}}_S(\nu,z_3^2)}{\mathcal{M}_{pp}(0,z_3^2)}\ . \tag{186}$$

The matching relation for the polarized gluon PDF is:

$$\begin{aligned}\widetilde{\mathfrak{M}}(\nu,z_3^2) &= \frac{\Delta\mathcal{I}_g(\nu,\mu^2)}{\mathcal{I}_g(0,\mu^2)}-\frac{\alpha_s C_A}{2\pi}\int_0^1 \mathrm{d}u\Bigg\{2\bar{u}u-\frac{1}{2}\delta(\bar{u})+4\left[\frac{u+\ln(1-u)}{\bar{u}}\right]_{+(1)}-\left[\frac{1}{\bar{u}}-\bar{u}\right]_{+(1)}\\ &\qquad +\ln\left(z_3^2\mu_{\mathrm{IR}}^2e^{2\gamma_E}/4\right)\widetilde{\mathcal{B}}_{gg}(u)\Bigg\}\frac{\Delta\mathcal{I}_g(u\nu,\mu^2)}{\mathcal{I}_g(0,\mu^2)}\\ &\quad -\frac{\alpha_s C_A}{2\pi}\int_0^1 \mathrm{d}u\left\{2\bar{u}u+\ln\left(z_3^2\mu_{\mathrm{IR}}^2e^{2\gamma_E}/4\right)\widetilde{\mathcal{B}}_{gq}(u)\right\}\frac{\Delta\mathcal{I}_S(\nu,\mu^2)}{\mathcal{I}_g(0,\mu^2)}\\ &\quad +\frac{\alpha_s C_A}{2\pi}\ln\left(z_3^2\mu_{\mathrm{IR}}^2e^{2\gamma_E}/4\right)\frac{4}{3}\frac{\mathcal{I}_S(0,\mu^2)}{\mathcal{I}_g(0,\mu^2)}\frac{\Delta\mathcal{I}_g(\nu,\mu^2)}{\mathcal{I}_g(0,\mu^2)}+\mathcal{O}\left(z_3^2m^2,z_3^2\Lambda_{\mathrm{QCD}}\right)\ . \end{aligned} \tag{187}$$

In a similar fashion to the unpolarized case, it is straightforward to rewrite Eq. (187) in terms of the lightcone polarized gluon PDF and polarized singlet quark PDF. Doing so leads

to the result:

$$\widetilde{\mathfrak{M}}(\nu, z_3^2) = \int_0^1 \mathrm{d}x \frac{x\Delta g(x,\mu^2)}{\langle x\rangle_{\mu^2}} \left(\widetilde{R}_{gg}(x\nu, z_3^2\mu^2) + \widetilde{R}_r(x\nu, z_3^2\mu^2) \frac{\langle x_S\rangle_{\mu^2}}{\langle x\rangle_{\mu^2}} \right) + \int_0^1 \mathrm{d}x \frac{x\Delta f_S(x,\mu^2)}{\langle x\rangle_{\mu^2}} \widetilde{R}_{gq}(x\nu, z_3^2\mu^2) + \mathcal{O}\left(z_3^2 m^2, z_3^2\Lambda_{\mathrm{QCD}}\right) \ , \tag{188}$$

where the R kernels in this case are given by the sine transform of the u dependent parts of Eq. (187). They are:

$$\widetilde{R}_{gg}(x\nu, z_3^2\mu^2) = \int_0^1 \mathrm{d}u \sin(ux\nu) \left(\delta(\bar{u}) - \frac{\alpha_s C_A}{2\pi} \left\{ 2\bar{u}u - \frac{1}{2}\delta(\bar{u}) + 4\left[\frac{u+\ln(1-u)}{\bar{u}}\right]_{+(1)} - \left[\frac{1}{\bar{u}} - \bar{u}\right]_{+(1)} + \ln\left(z_3^2\mu_{\mathrm{IR}}^2 e^{2\gamma_E}/4\right) \widetilde{\mathcal{B}}_{gg}(u) \right\} \right) \ , \tag{189}$$

$$\widetilde{R}_{gq}(x\nu, z_3^2\mu^2) = \int_0^1 \mathrm{d}u \sin(ux\nu) \left(-\frac{\alpha_s C_A}{2\pi} \left\{ 2\bar{u}u + \ln\left(z_3^2\mu_{\mathrm{IR}}^2 e^{2\gamma_E}/4\right) \widetilde{\mathcal{B}}_{gq}(u) \right\} \right) \ , \tag{190}$$

$$\widetilde{R}_r(x\nu, z_3^2\mu^2) = \frac{4}{3}\sin(x\nu)\frac{\alpha_s C_A}{2\pi} \ln\left(z_3^2\mu_{\mathrm{IR}}^2 e^{2\gamma_E}/4\right) \ . \tag{191}$$

Because the ratio in this case was constructed with the unpolarized result, $\langle x_S\rangle_{\mu^2}$ and $\langle x\rangle_{\mu^2}$ appear again in the polarized matching relation.

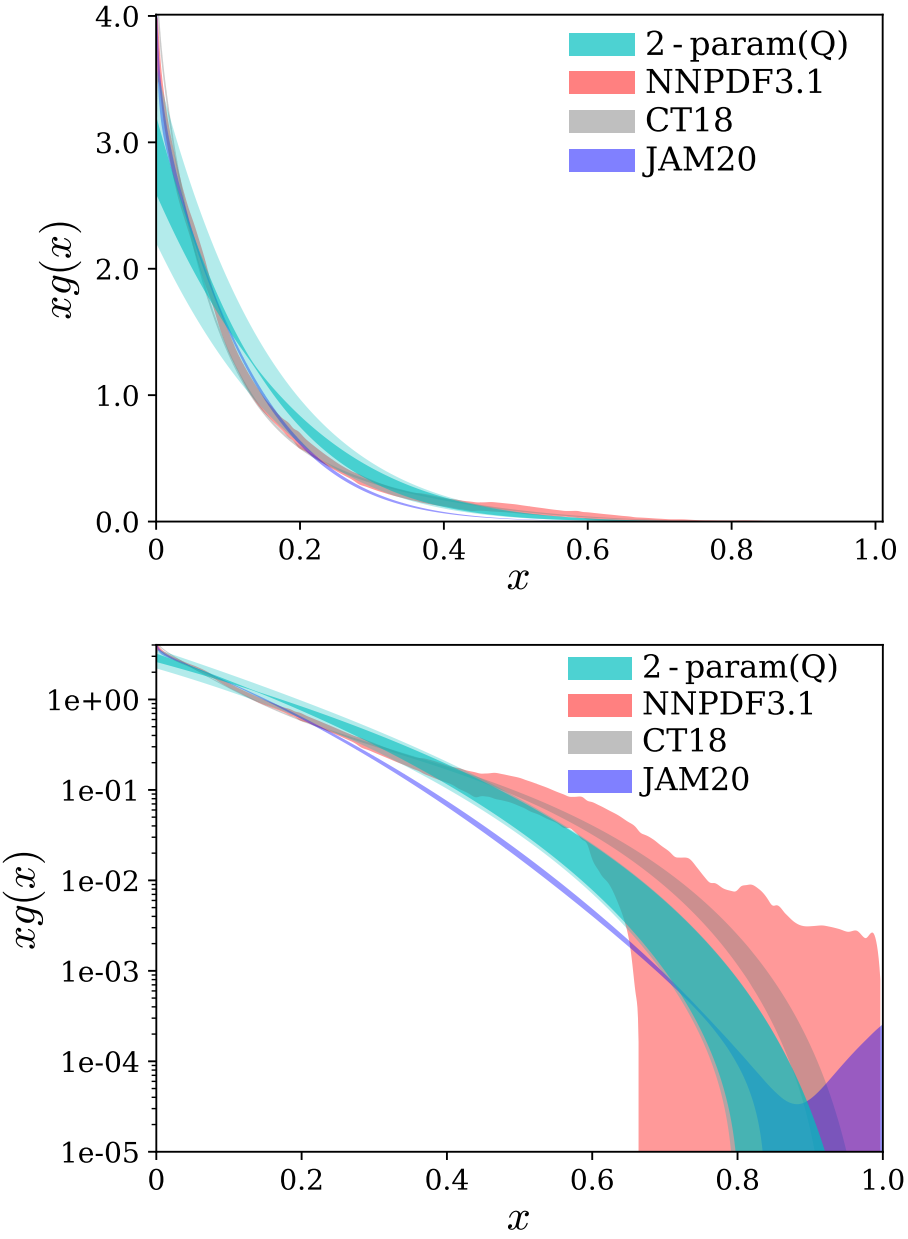

FIG. 9: Unpolarized gluon PDF (cyan band) extracted from HadStruc lattice data using the 2-param (Q) model. Results are compared to gluon PDFs extracted from global fits to experimental data, CT18 [31], NNPDF3.1 [32], and JAM20 [33]. The gluon momentum fraction used in the calculation was $\langle x \rangle_{\mu^2=4\,\mathrm{GeV}^2} = 0.427(92)$ from [34]. The bottom figure uses a logarithmic scale in order to enhance the view of the large-x region. [35]

CHAPTER 7
CONCLUSIONS

In this dissertation the methods of computation of one-loop corrections to the gluon bilocal operator were outlined. Specifically, the external field method, and the heat-kernel expansion. The results of the calculation were discussed, along with some of the features of the calculation that are unique to the methods applied. Additionally, the one-loop calculation of the gluon-quark operator mixing contribution was given. A discussion of the logarithmic UV and IR behavior of the various contributions was given, and the UV anomalous dimensions associated with the various multiplicatively renormalizable projections of the gluon operator were calculated.

The application of the gluon bilocal operator to forward matrix elements was discussed, along with the key differences between the result at spacelike and lightlike seperations.

Finally, the application of the unpolarized and polarized forward matrix elements to the method of pseudodistributions was discussed. Specifically, the matching relation between pseudo-ITDs and lightcone PDFs was given in for unpolarized and polarized cases. These matching relations have already been used in the lattice extraction of light cone PDFs by the HadStruc collaboration at Jefferson Lab [35], and the lattice group at Michigan State University [37, 38]. Again, these are the results of the calculation of the gluon PDF from first principles in QCD. Future improvements to the lattice extraction of the gluon PDF should incorporate the gluon-quark mixing, and should ideally include greater values of the Ioffe-time, ν.

Once again, a key feature of the general result for the gluon bilocal operator is its process independence, and therefore its applicability to nonforward matrix elements. With that in mind, this result can be used in the future calculation of matching conditions for the extraction of gluon GPDs and DAs from lattice calculations, in addition to other distributions that may not be experimentally accessible.

BIBLIOGRAPHY

[1] M. Gell-Mann, Physics Letters **8**, 214 (1964).

[2] G. Zweig, Developments in the Quark Theory of Hadrons **1** (1980).

[3] R. P. Feynman, Phys. Rev. Lett. **23**, 1415 (1969).

[4] J. D. Bjorken, Phys. Rev. **179**, 1547 (1969).

[5] J. D. Bjorken and E. A. Paschos, Phys. Rev. **185**, 1975 (1969).

[6] E. D. Bloom *et al.*, Phys. Rev. Lett. **23**, 930 (1969).

[7] M. Breidenbach, J. I. Friedman, H. W. Kendall, E. D. Bloom, D. H. Coward, H. C. DeStaebler, J. Drees, L. W. Mo, and R. E. Taylor, Phys. Rev. Lett. **23**, 935 (1969).

[8] C. N. Yang and R. L. Mills, Phys. Rev. **96**, 191 (1954).

[9] D. J. Gross and F. Wilczek, Phys. Rev. Lett. **30**, 1343 (1973).

[10] K. G. Wilson, Phys. Rev. D **10**, 2445 (1974).

[11] X. Ji, Phys. Rev. Lett. **110**, 262002 (2013).

[12] A. V. Radyushkin, Phys. Rev. D **96**, 034025 (2017).

[13] B. DeWitt, *Dynamical Theory of Groups and Fields* (Gordon and Breach, New York, 1965).

[14] I. Balitsky and V. Braun, Nuclear Physics B **311**, 541 (1989).

[15] J. Beringer *et al.* (Particle Data Group), Phys. Rev. D **86**, 010001 (2012).

[16] V. Gribov and L. Lipatov, Yadern. Fiz **15**, 1218 (1972).

[17] Y. L. Dokshitzer, JETP **46**, 461 (1977).

[18] G. Altarelli and G. Parisi, Nuclear Physics B **126**, 298 (1977).

[19] V. Braun, P. Górnicki, and L. Mankiewicz, Phys. Rev. D **51**, 6036 (1995).

[20] B. Ioffe, Physics Letters B **30**, 123 (1969).

[21] K. Orginos, A. Radyushkin, J. Karpie, and S. Zafeiropoulos, Phys. Rev. D **96**, 094503 (2017), arXiv:1706.05373 [hep-ph] .

[22] A. V. Radyushkin, Phys. Rev. D **96**, 034025 (2017).

[23] I. Balitsky, W. Morris, and A. Radyushkin, Phys. Lett. B **808**, 135621 (2020), arXiv:1910.13963 [hep-ph] .

[24] I. Balitsky, W. Morris, and A. Radyushkin, Phys. Rev. D **105**, 014008 (2022), arXiv:2111.06797 [hep-ph] .

[25] I. Balitsky, W. Morris, and A. Radyushkin, Journal of High Energy Physics **2022**, 193 (2022).

[26] A. Radyushkin, Phys. Rev. D **98**, 014019 (2018), arXiv:1801.02427 [hep-ph] .

[27] J.-H. Zhang, J.-W. Chen, and C. Monahan, Phys. Rev. D **97**, 074508 (2018).

[28] T. Izubuchi, X. Ji, L. Jin, I. W. Stewart, and Y. Zhao, Phys. Rev. D **98**, 056004 (2018).

[29] J.-H. Zhang, X. Ji, A. Schäfer, W. Wang, and S. Zhao, Phys. Rev. Lett. **122**, 142001 (2019).

[30] A. Polyakov, Nuclear Physics B **164**, 171 (1980).

[31] T.-J. Hou, J. Gao, T. J. Hobbs, K. Xie, S. Dulat, M. Guzzi, J. Huston, P. Nadolsky, J. Pumplin, C. Schmidt, I. Sitiwaldi, D. Stump, and C.-P. Yuan, Phys. Rev. D **103**, 014013 (2021).

[32] R. D. Ball, V. Bertone, S. Carrazza, L. D. Debbio, S. Forte, P. Groth-Merrild, A. Guffanti, N. P. Hartland, Z. Kassabov, J. I. Latorre, E. R. Nocera, J. Rojo, L. Rottoli, E. Slade, and M. Ubiali, The European Physical Journal C **77**, 663 (2017).

[33] E. Moffat, W. Melnitchouk, T. C. Rogers, and N. Sato (Jefferson Lab Angular Momentum (JAM) Collaboration), Phys. Rev. D **104**, 016015 (2021).

[34] C. Alexandrou, S. Bacchio, M. Constantinou, J. Finkenrath, K. Hadjiyiannakou, K. Jansen, G. Koutsou, H. Panagopoulos, and G. Spanoudes (Extended Twisted Mass Collaboration), Phys. Rev. D **101**, 094513 (2020).

[35] T. Khan *et al.* (HadStruc), Phys. Rev. D **104**, 094516 (2021), arXiv:2107.08960 [hep-lat] .

[36] R. S. Sufian, T. Liu, and A. Paul, Phys. Rev. D **103**, 036007 (2021).

[37] Z. Fan and H.-W. Lin, Physics Letters B **823**, 136778 (2021).

[38] Z. Fan, R. Zhang, and H.-W. Lin, International Journal of Modern Physics A **36**, 2150080 (2021).

[39] L. Faddeev and V. Popov, Physics Letters B **25**, 29 (1967).

APPENDIX A
LIGHTCONE VARIABLES

Lightcone variables are incredibly convenient to work with in high energy processes, where the object under consideration is typically boosted in a specific direction. A vector, A, in lightcone variables is given by:

$$A^{\pm} = \frac{A^0 \pm A^3}{\sqrt{2}} \ , \quad \mathbf{A}_{\perp} = \left(A^1, A^2\right) \ . \tag{192}$$

The presence of the $\sqrt{2}$ in the definition of $A^{\pm}$ leads to a definition of the metric tensor where:

$$g_{\mu\nu} = g^{\mu\nu} = \begin{pmatrix} 0 & 1 & 0 & 0 \\ 1 & 0 & 0 & 0 \\ 0 & 0 & -1 & 0 \\ 0 & 0 & 0 & -1 \end{pmatrix} \ , \tag{193}$$

then the scalar product has the form:

$$(AB) = A^+B^- + A^-B^+ - (\mathbf{A}_{\perp}\mathbf{B}_{\perp}) \tag{194}$$

$$A^2 = 2A^+A^- - \mathbf{A}_{\perp}^2 \tag{195}$$

Lorentz boosts along the 3 direction take on a simple form in lightcone variables:

$$A'^{+} = A^+e^{\zeta} \ , \qquad A'^{-} = A^-e^{-\zeta} \ , \qquad \mathbf{A}'_{\perp} = \mathbf{A}_{\perp} \ , \tag{196}$$

where ζ is a hyperbolic angle defined in terms of the frame velocity:

$$\zeta = \frac{1}{2}\ln\frac{1+v}{1-v} \ . \tag{197}$$

APPENDIX B
OVERVIEW OF QCD

Quantum chromodynamics is based on SU(3), non-Abelian gauge theory and describes the interaction between massive spin-$\frac{1}{2}$ fermions called quarks and massless vector gauge bosons called gluons. The full QCD Lagrangian is:

$$\mathcal{L}_{\text{QCD}} = \mathcal{L}_{\text{GI}} + \mathcal{L}_{\text{GF}} + \mathcal{L}_{\text{ghost}} \ , \tag{198}$$

where the first term on the RHS is the SU(3) gauge invariant part describing the quark and gluon fields. The second and third terms are the gauge fixing and ghost terms, respectively.

B.1 Gauge invariant term

The gauge invariant term is, with all indices made explicit:

$$\mathcal{L}_{\text{GI}} = \sum_{f=1}^{n_f} \bar{\psi}_f^i \left(i\gamma^\mu D_\mu - m_f \right)^{ij} \psi_f^j - \frac{1}{4} G_{\mu\nu}^a G^{a,\mu\nu} \ . \tag{199}$$

The quark fields, ψ_f^j, exist in the fundamental representation of SU(3), while their adjoint counterparts, $\bar{\psi}_f^i$ are dual vectors, with elements denoted by the indices $i, j \in \{1, 2, 3\}$. The index, f, denotes a sum over the number of quark flavors, n_f, with the flavor specific quark masses m_f. The covariant derivative in the quark term is defined as:

$$D_\mu = \partial_\mu - igt^a A_\mu^a \ , \tag{200}$$

where A_μ^a are the gluon gauge fields, and t^a are the eight SU(3) group generators in the fundamental representation. They have the algebra:

$$\left[t^a, t^b \right] = i f^{abc} t^c \ , \tag{201}$$

$$\text{Tr}\, t^a t^b = T_F \delta^{ab} \ , \tag{202}$$

$$t^a t^b = C_F I_{3\times 3} = \frac{N^2-1}{2N} I_{3\times 3} \ . \tag{203}$$

Where C_F is the Casimir operator, and $N = 3$ in an SU(3) theory, while $T_F = \frac{1}{2}$.

The gluon field strength tensor, $G^a_{\mu\nu}$, is a vector in the adjoint representation of SU(3) with elements indicated by index $a \in \{1, 2, 3, 4, 5, 6, 7, 8\}$, and is defined by:

$$G_{\mu\nu} = T^a G^a_{\mu\nu} = i\left[D_\mu, D_\nu\right] \ , \tag{204}$$

$$D_\mu = \partial_\mu - igT^a A^a_\mu \ , \tag{205}$$

where D_μ is the covariant derivative in the adjoint representation, A_μ is the gluon gauge field, and T^a are the gauge group generators in the adjoint representation with algebra:

$$\left[T^a, T^b\right] = if^{abc}T^c \tag{206}$$

$$T^a T^a = C_A I_{8\times 8} \ , \tag{207}$$

$$\mathrm{Tr}\, T^a T^b = T_A \delta^{ab} = C_A \delta^{ab} \ , \tag{208}$$

where in the usual QCD the adjoint Casimir operator, C_A is equal to 3, the number of colors charges in the theory.

The gluon and quark fields undergo infinitesimal transformations in the local SU(3) gauge group:

$$\psi \to (1 + i\alpha^a t^a)\,\psi \ , \tag{209}$$

$$A_\mu \to A_\mu + \frac{1}{g}\left[D_\mu, \alpha^a T^a\right] \ . \tag{210}$$

Applying Eqs. (209) and (210) to $\mathcal{L}_{\mathrm{GI}}$ leaves it invariant, as the name suggests.

B.2 Gauge fixing term

In QCD it is necessary to introduce a gauge fixing term in order to account for the unphysical degrees of freedom in the theory. A common choice are the R_ξ gauges, given by:

$$\mathcal{L}_{\mathrm{GF}} = -\frac{1}{2\xi}\left(\partial^\mu A^a_\mu\right)^2 \ , \tag{211}$$

where ξ is an arbitrary parameter. The case where $\xi = 1$ is called the Feynman 't Hooft gauge. Another common gauge choice is the axial gauge:

$$\mathcal{L}_{\mathrm{GF}} = n^\mu A^a_\mu \ , \tag{212}$$

where n^μ is some vector. A common choice in this case is the lightcone gauge where $n^\mu = (n^+, 0, 0_\perp)$ in the lightcone coordinates. The lightcone gauge greatly simplifies the calculation of the parton level lightcone PDFs.

B.3 Ghost term

The ghost term, given by:

$$\mathcal{L}_{\mathrm{ghost}} = \partial^\mu \bar{\eta}^a D^{ab}_\mu \eta^b \ , \tag{213}$$

describes the Faddeev-Popov ghost fields [39], η^a, that are associated with the gluon. The covariant derivative in this case is in the adjoint representation with the matrix indices made explicit. The ghost term is necessary to compensate the gauge fixing term in the Feynman-'t Hooft gauge, and in the background field gauge. However, in the case of the axial gauges the ghost fields uncouple from the theory.

VITA

Wayne Henry Morris III

Department of Physics, Old Dominion University

306 Oceanography and Physics Building

4600 Elkhorn Ave, Norfolk, VA 23529

Education:

Old Dominion University, Norfolk, VA

M.S. Physics, May 2017

James Madison University, Harrisonburg, VA

B.S. Physics, May 2015

Research Experience:

2017-Present Research Assistant, Old Dominion University, Norfolk, VA

2019-Present Member of HadStruc Collaboration, Jefferson Lab, Newport News, VA

2013-2015 Research Assistant, James Madison University, Harrisonburg, VA

Selected publications:

1. I. Balitsky, W. Morris, A. Radyushkin. Polarized gluon pseudodistributions at short distances. JHEP 2022, 193 (2022). arXiv:2112.02011v1.

2. C. Egerer, et al. 2021. The transversity parton distribution function of the nucleon using the pseudo-distribution approach. Phys. Rev. D 105, 034507 (2022). arXiv:2111.01808v1.

3. I. Balitsky, W. Morris, A. Radyushkin. 2021. Short-distance structure of unpolarized gluon pseudodistributions. Phys. Rev. D 105, 014008 (2022). arXiv:2111.06797v1.

4. T. Khan, et al. 2021. Unpolarized gluon distribution in the nucleon from lattice quantum chromodynamics. Phys. Rev. D 104, 094516 (2021). arXiv:2107.08960v2.

5. I. Balitsky, W. Morris, A. Radyushkin. 2020. Gluon pseudo-distributions at short distances: Forward case. Physics Letters B 808, 135621 (2020). arXiv:1910.13963v3.

Typeset using LaTeX.